

Maternal and Fetal Toxicity of Carisoprodol

Magdy H. Abouel-Magd

Narcotic Research Department, the National Center for Social and Criminological Research, Cairo, Egypt

ABSTRACT

Aim of the work: this study aimed to detect the histological and histochemical changes in liver tissue of pregnant rats and their fetuses after treatment with carisoprodol. **Material and methods:** thirty pregnant female rats were randomly categorized into three groups (ten pregnant female rats in each group). The first was administered oral doses of distilled water and was served as control. The other two groups were administered oral doses of carisoprodol in the distilled water equivalent to 10.8 mg and 21.6 mg/100g body weight/day respectively for 15 days from the 6th day to the 20th day of gestation. Numerous histological and histochemical studies were done to detect the histopathological and histochemical changes. **Results:** maternal and fetal liver tissue of both treated groups showed lots of degenerative changes post-treatment with carisoprodol. The severity of these changes was more obvious in fetal liver tissue of both groups this was accompanied with numerous histochemical changes. **Conclusion:** treatment of pregnant rats with carisoprodol led to numerous dystrophic changes in maternal and fetal liver tissue.

Keywords: carisoprodol, mammals, pregnant rats, fetuses, histopathology and histochemistry.

INTRODUCTION

Carisoprodol (N-isopropyl-2 methyl-2-propyl-1,3-propanediol dicarbamate; N-isopropyl-meprobamate) is a commonly prescribed centrally acting skeletal muscle relaxant indicated as adjunct therapy to rest, physiotherapy and other measures for the relief of discomfort related to painful musculoskeletal conditions in adults ⁽¹⁾. The drug is widely used in primary care settings. Carisoprodol compound is marketed under a variety of brand names such as Somadril, Soma, Somalgit, Vanadam, Sodal, Carisoma, Sonoma, Somacid, Scutamil C, Relacton-C, Mio Relax, Relaxibys, Rela and Soridol ⁽²⁾.

Carisoprodol (molecular formula $C_{12}H_{24}N_2O_4$, molecular weight $260.33 \text{ g mol}^{-1}$) is a white crystalline powder that has a mild characteristic odor and a bitter taste. Carisoprodol begins to act within 30 minutes of oral ingestion and has a half-life of approximately 1.5 hours. Adverse effects of carisoprodol mainly involve the central nervous system (CNS) and include drowsiness, dizziness, ataxia, tremor, blurred vision and headache ⁽³⁾. Carisoprodol is converted to three primary metabolites in the liver: hydroxyl carisoprodol, hydroxyl meprobamate and meprobamate ⁽²⁾, which are excreted by the kidneys ⁽⁴⁾. The exact mechanism of action of carisoprodol is unknown, but the drug is thought to act centrally by causing sedation rather than by direct skeletal muscle relaxation; it may act by inhibiting interneuron transmission in the descending reticular formation and spinal cord ⁽⁵⁾. A part of the apparent effect of carisoprodol may be due to the meprobamate metabolite which has a half-life of approximately 11 hours (Although this may be prolonged to up to 48 hours with chronic usage) ⁽⁶⁾.

There is an evidence that meprobamate produces its clinical effects by barbiturate like activating activity at GABAA receptors {The GABA receptors are a class of receptors that respond to the neurotransmitter gamma-aminobutyric acid} ⁽⁷⁾. A research had showed that carisoprodol itself may activate GABAA receptors independent of the action of meprobamate ⁽⁸⁾. How much of the clinical effect observed in a patient taking carisoprodol is due to carisoprodol alone and how much is contributed by the meprobamate metabolite is not currently known. In Egypt, carisoprodol is available as somadril compound which contains carisoprodol 200mg, paracetamol 160mg and caffeine 32mg. It is a prescribed drug produced by Mina Pharm for pharmaceutical regulations by the decision of the Minister of Health and Population No.172 of the year 2011, while meprobamate the active metabolite of carisoprodol ⁽⁹⁾ is a schedule 111 controlled substance on Anti-drug law No. 182 of the year 1960. Carisoprodol has a narrow therapeutic range ⁽¹⁰⁾ and when carisoprodol is ingested with other medications it may be a contributing factor in death, even when present at therapeutic concentrations ⁽¹¹⁾. Paracetamol (Acetaminophen) is widely used over the counter drug for analgesic and antipyretic effects. Its use in suicidal or accidental or with chronic alcohol abuse causes fulminant liver failure ⁽¹²⁾. Paracetamol induced hepatic failure is the second leading cause of liver transplantation ⁽¹³⁾. Caffeine is a central nervous system and metabolic stimulant and is used both recreationally and medically to reduce physical fatigue and to restore alertness when drowsiness occurs ⁽¹⁴⁾. Caffeine overdose can result in a state of central nervous system over-stimulation called caffeine intoxication ⁽¹⁵⁾. Liver injury caused by toxic chemicals and

certain drugs has been recognized as a toxicological problem. Hepatotoxicity is one of a very common ailment resulting into serious changes ranging from severe metabolic disorders to even mortality⁽¹⁶⁾.

Carisoprodol (Somadril compound) is a muscle relaxant antispasmodic that indicated for the relief of discomfort associated with acute, painful musculoskeletal conditions in adults⁽¹⁷⁾. No available researches were obtained which concerning the histological and histochemical changes in the mammalian tissues post-Somadril treatment. This work aimed to study the effect of carisoprodol compound drug on the maternal and fetal liver of Albino rats.

MATERIAL and METHODS

Drug

Carisoprodol compound: carisoprodol tablets (Somadril compound) is indicated for the relief of discomfort associated with acute, painful musculoskeletal conditions in adults. Carisoprodol compound drug was obtained as tablets of a combination product containing carisoprodol 200mg, paracetamol 160mg and caffeine 32mg, it is obtained from Mina Pharm for Pharmaceuticals and Chemical Industries, Cairo, A.R.E.

Animals

Adult Sprague Dawley male and female albino rats were used in this experiment, with average weight 150- 200g. They were taken from the Animal House of El-Nasr Pharmaceutical Chemicals Co. Animals were caged separately, males in cages and females in others. All rats were housed in a quite non-stressful environment for one week before beginning the present study.

They were offered normal rat chows and water *ad libitum* during the experimental period. Female rats were mated in the proportion of 2 females for one male overnight. Each morning a vaginal smear was taken to check for the presence of sperms or plug in the vagina. Zero day of pregnancy was considered to be the day on which Sperms or plug were found in the vagina. Thirty pregnant female rats were randomly categorized into three groups (ten pregnant female rats in each group). The first was administered oral doses of distilled water and was served as control. The other two groups (**S1 and S2**) were administered oral doses of carisoprodol in the distilled water equivalent to 10.8 mg and 21.6 mg/100g body weight/day respectively for 15 days from the 6th day to the 20th day of gestation.

The dose for rats was calculated according to the method **Paget and Barnes**⁽¹⁸⁾ formula on the basis

of the human dose. All groups were sacrificed after 4 hours from the last drug administration.

Histopathological examination

All pregnant rats were sacrificed and small pieces of placenta and liver from mothers and their fetuses were picked out, rinsed in formalin (10%) and Bouin's solution for the histological and histochemical purposes. Sections of placenta and liver from mothers and their fetuses were prepared and stained with hematoxylin and eosin stain according to the method reported by **Bancroft and Gamble**⁽¹⁹⁾. Total proteins were detected by using mercuric bromophenol blue method⁽²⁰⁾, polysaccharides were detected by using periodic acid Schiff's (PAS) reagent⁽²¹⁾ and collagen fibres were stained by using Mallory's trichrome stain method⁽²²⁾. Amyloid protein was detected by Congo red technique⁽²³⁾. DNA was detected by using Feulgen reaction⁽²¹⁾.

Statistical analysis

Statistical analyses were performed using analyses of variance (ANOVA) according to the method **Jaeger**⁽²⁴⁾. The data were processed and analyzed using the SPSS software (Statistical Analysis for Social Science, Version 8). Significant differences between treatment means were determined by student T-test. Data were presented as mean±SE and $P \leq 0.05$ was considered statistically significant.

RESULTS

Results of the pregnant rats

Fig.1 showed cords of hepatocytes which were surrounding the central vein in the hepatic tissue of a control pregnant rat with sinusoidal spaces in between the hepatocytes and Kupffer cells. **Figures 2-6** showed numerous degenerative changes in liver tissue of pregnant rats of **group S1**. These changes included: highly congested and dilated central veins and blood sinusoids, hemosiderin granules and hemolysed blood cells inside the hepatic portal veins, highly thickened arterial walls in the portal areas, highly distorted portal areas, some hepatocytes were vacuolated and contained pyknotic or karyolytic nuclei. Liver tissue of pregnant rats of **group S2 (Figures 7-9)** showed many dystrophic changes. These changes included: delaminated endothelial lining of the central veins, vacuolated hepatocytes with pyknotic nuclei, highly elongated and distorted walls of the bile ducts, large hemorrhagic areas and numerous fibroblasts in the portal areas.

Thin collagen fibers were supporting walls of hepatocytes, blood vessels, blood sinusoids of the liver tissue of a control pregnant rat (**Fig.10**). Highly increased collagen fibers were detected in liver tissue of pregnant rats of **group S1 (Figures 11-13)** especially in walls of the bile ducts, blood vessels, hepatocytes and in the distorted portal areas with brightly red stained hemorrhagic areas and aggregated RBCs in the congested blood sinusoids. Also, highly increased collagen fibers were detected in liver tissue of pregnant rats of **group S2 (Figures 14&15)**.

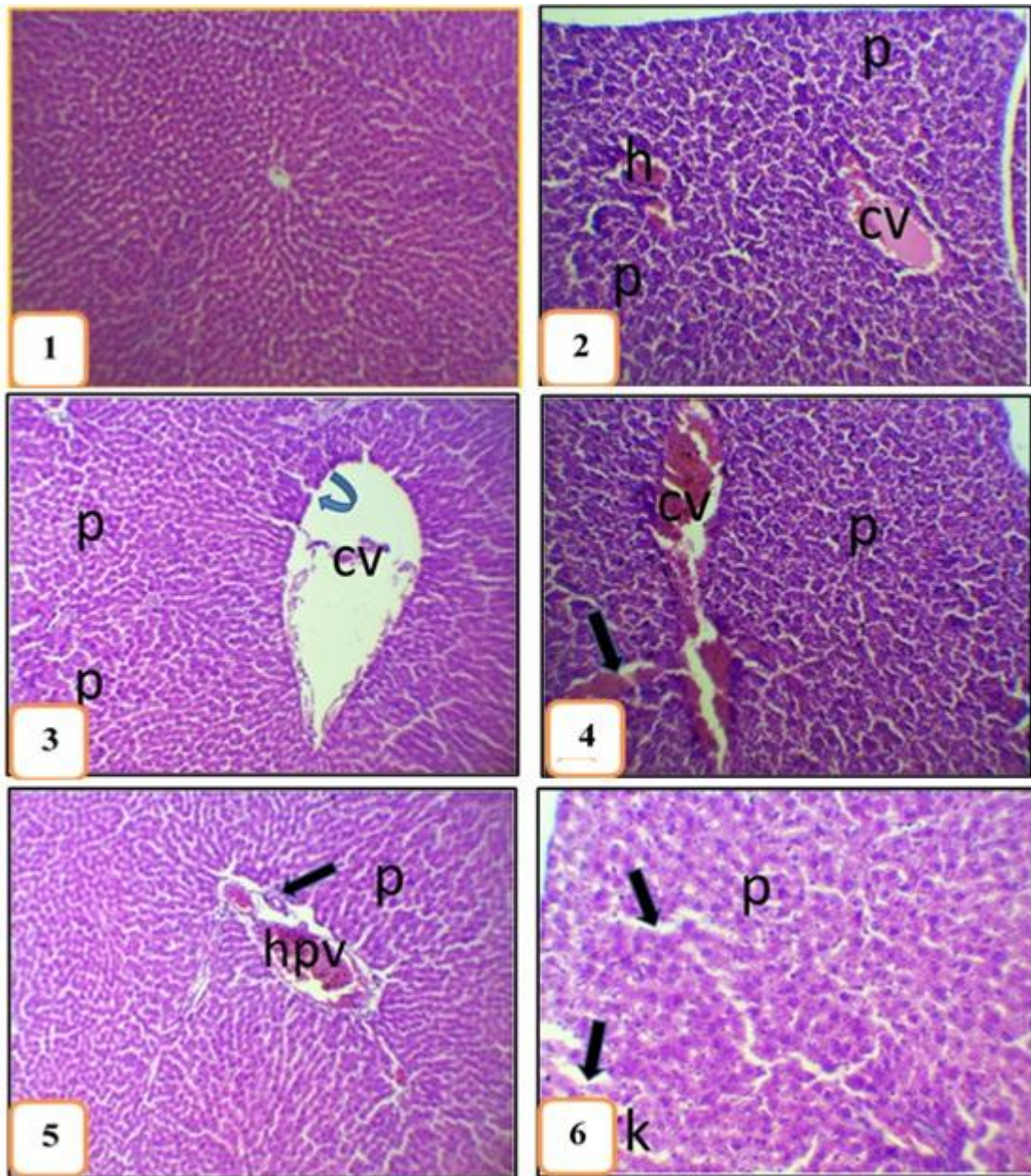
Fig.16 showed moderately stained total protein in liver tissue of a control pregnant rat. **Figures 17&18** showed decreased total protein in liver tissue of rats of **group S1**; optical density reached 0.53 ± 0.06 in comparison with the control group (0.85 ± 0.08). Also, reduced total protein was detected in liver tissue of **group S2**, but increased staining affinity was realized in blood cells inside the congested hepatic portal vein and walls of the bile ducts (**Figures 19&20**). Optical density reached 0.44 ± 0.03 (**Table1 and fig. 21**).

Fig. 22: showed normal distribution of polysaccharides in the liver tissue of the control pregnant rat. **Figures 23&24** showed reduced polysaccharides in the liver tissue of rats of **group S1**; optical density reached 0.27 ± 0.02 in comparison with the control group (0.70 ± 0.06). Also, highly depleted PAS+ve materials were realized in most hepatocytes of the liver tissue of **group S2 (Figures**

25&26). Optical density reached 0.35 ± 0.02 in comparison with the control group (**Table2 and fig.27**). **Fig.28** showed faintly stained amyloid-B protein in liver tissue of a control pregnant rat.

Figures 29&30 showed increased amyloid deposits in liver tissue of **S1 group** especially in hepatocytes of the cortical region, in the delaminated epithelial lining of the hepatic portal vein, in the arterial wall, in walls of the bile ducts and inside the blood vessels; optical density reached 1.00 ± 0.11 in comparison with the control group (0.21 ± 0.01). Also, deeply stained amyloid deposits were observed in most hepatocytes of the portal and central areas, inside the congested artery, in walls of the bile ducts and blood vessels of the liver tissue of **group S2 (Figures 31&32)** optical density reached 1.16 ± 0.11 in comparison with the control group (**Table3 and fig.33**).

Fig. 34 showed moderately stained nuclei of hepatocytes in liver tissue of a control pregnant rat stained with Feulgen reaction to detect DNA materials. **Figures 35&36** showed highly reduced DNA materials in most nuclei of hepatocytes, in the central and portal areas in the liver tissue of pregnant rats of **group S1**; optical density reached 0.16 ± 0.02 in comparison with the control group (0.83 ± 0.03). Also, decreased DNA materials were realized in most nuclei of hepatocytes, in the central and portal areas in the liver tissue of pregnant rats of **group S2 (Figures 37&38)** optical density reached 0.31 ± 0.02 in comparison with the control group (**Table4 and fig.39**).



Figures 1-9: photomicrographs of liver tissue of the pregnant rats of the control and treated groups stained with hematoxylin and eosin.

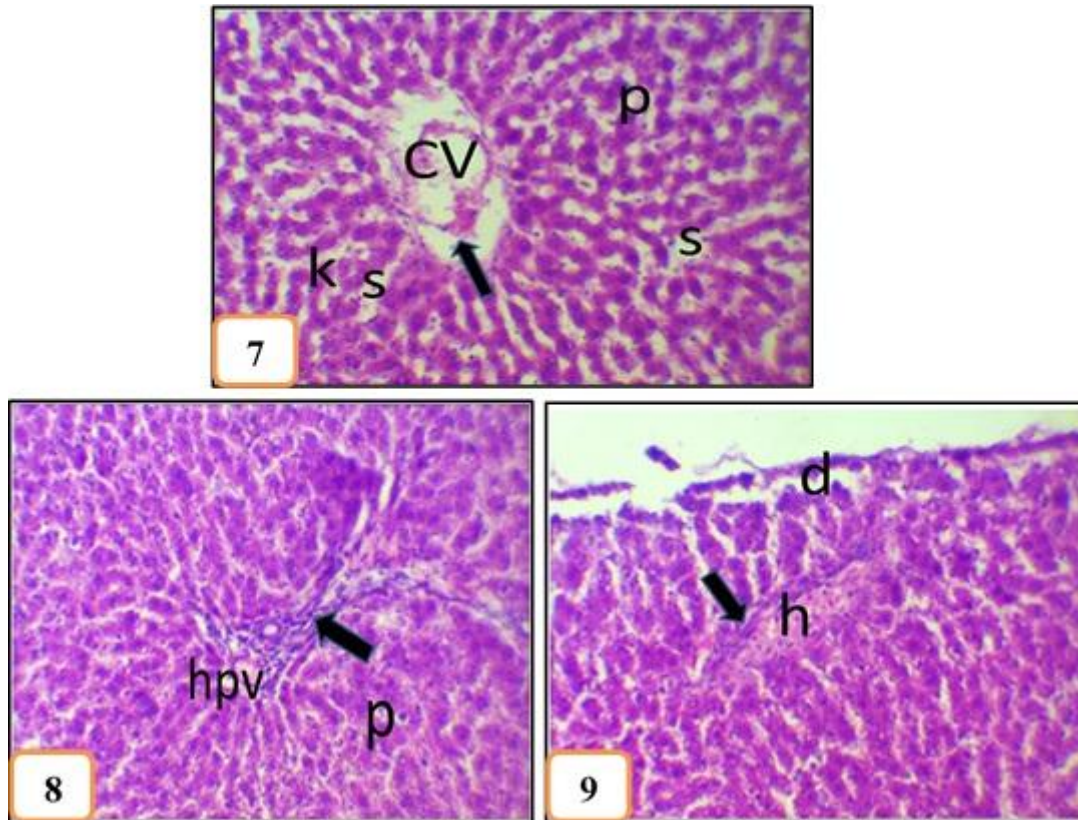
Fig.1: showing cords of hepatocytes which are surrounding the central vein and sinusoidal spaces in between them in liver of a control rat. (X100)

Figures 2-6 (S1): showing liver tissue of pregnant rats of **group S1** stained with hematoxylin and eosin.

Figures 2-4: showing highly dilated and congested central vein (cv), delaminated endothelial lining of the central vein (↷), numerous hemorrhagic areas (h), highly dilated and congested blood sinusoids (➔) with numerous darkly stained nuclei of hepatocytes (Pyknotic, p) of the liver tissue of S1group. Notice: hemolysed blood cells and hemosiderin granules inside the dilated and congested hepatic portal vein (hpv). (X200)

Fig.5: showing numerous pyknotic nuclei of hepatocytes (p), highly distorted portal area which contains highly thickened arterial wall and highly destructed walls of the bile ducts (➔). (X200)

Fig.6: showing numerous degenerative changes in the cortical hepatocytes and highly dilated sinusoidal spaces (➔). Notice: pyknosis (p) and karyolysis (k) in some nuclei of hepatocytes with numerous vacuolated hepatocytes. (X200)

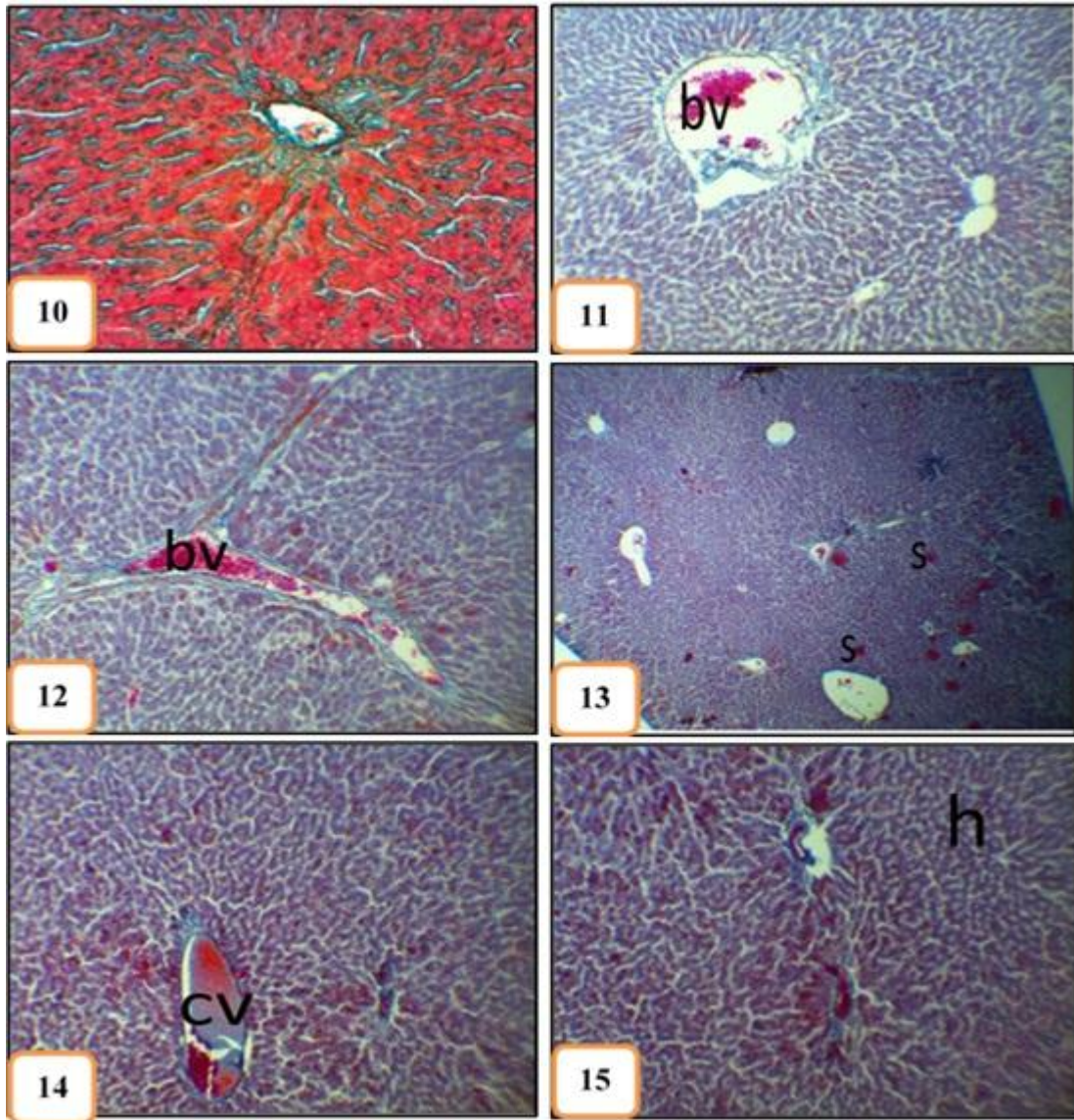


Figures 7-9 (S2): photomicrographs of liver tissue of the pregnant rats of group **S2** stained with hematoxylin and eosin

Fig.7: showing delaminated endothelial lining of the central vein (C V), which contains hemolysed blood cells (➡), numerous pyknotic (p) or karyolytic (k) nuclei of hepatocytes with highly dilated sinusoidal spaces (S). (X250)

Fig.8: showing highly distorted portal area which contains distorted hepatic portal vein (hpv), the bile ducts lost their normal architecture with lymphocytic infiltration (➡) and appearance of some vacuolated hepatocytes which contain pyknotic nuclei (p). (X250)

Fig.9: showing large hemorrhagic area (h), which is surrounded by numerous fibroblasts (➡) with numerous degenerated hepatocytes (d) especially under the capsule. (X250)

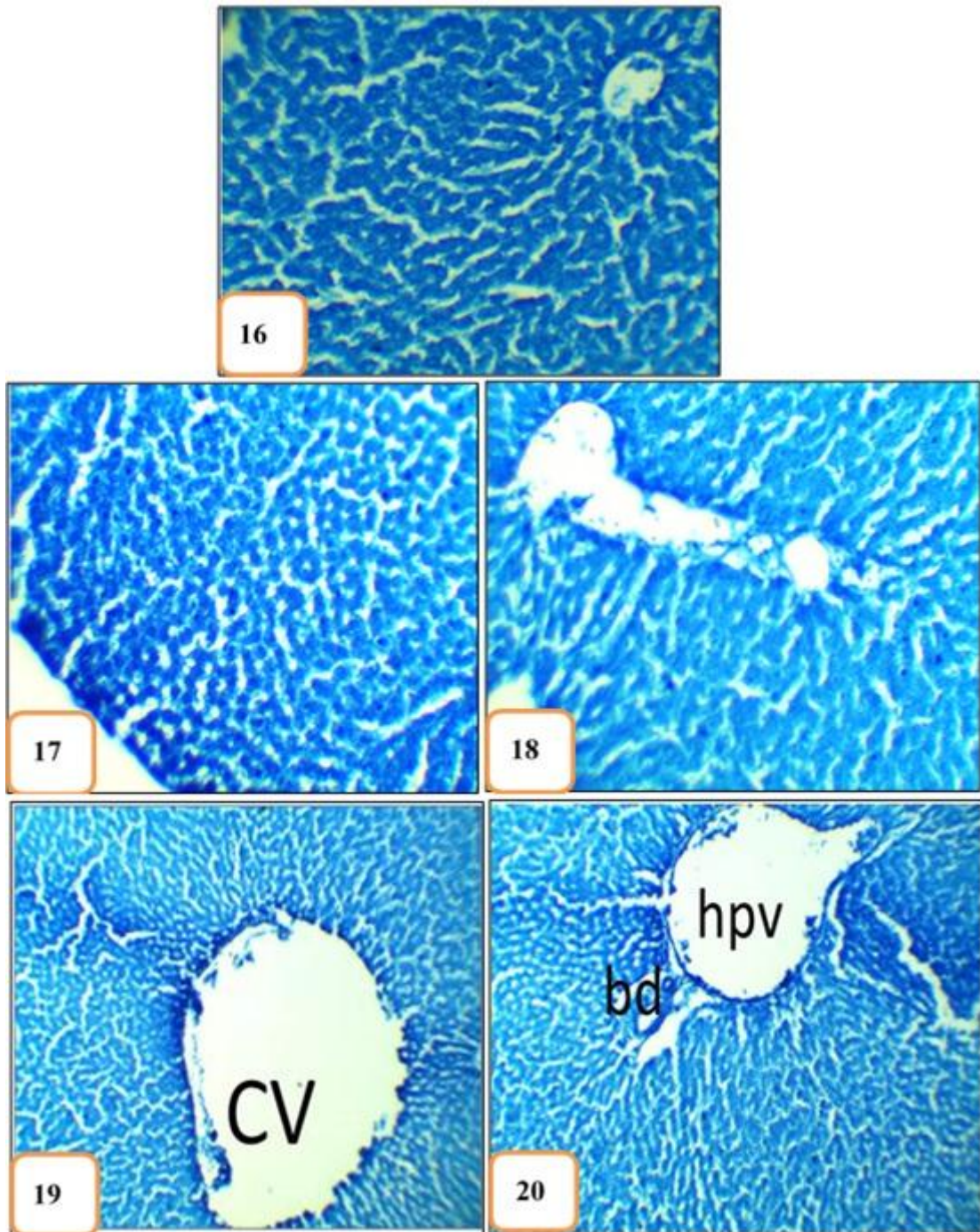


Figures 10-15: photomicrographs of the liver tissue of the control and treated groups stained with Mallory's trichrome stain for detection of collagen fibres.

Fig.10: showing thin bundles of collagen fibres support walls of hepatocytes, blood sinusoids and walls of the blood vessels in the liver tissue of a control rat. (X200)

Figures 11-13 (S1): showing highly increased collagen fibres in the liver tissue of S1 group especially in the hepatocytes, walls of the blood vessels (bv), bile ducts and in the portal areas. Notice: brightly red stained hemorrhagic areas and aggregated RBCs in the congested blood sinusoids (S), especially in the cortical regions. (11&12X200 &13X100)

Figures 14&15 (S2): showing highly increased collagen fibres in the liver tissue of S2 group especially in and around the congested central vein, in the portal area and in walls of the hepatocytes (h). Notice: brightly red stained blood cells in the congested blood vessels and the congested blood sinusoids. (X200)



Figures 16-20: photomicrographs of the liver tissue of the control and treated groups of the pregnant rats showing total protein stained with mercuric bromophenol blue.

Fig.16: showing moderately stained total protein content in the liver tissue of the control pregnant rat.

(X200)

Figures 17&18 (S1): showing reduced staining affinity of total protein in some hepatocytes of the central and portal areas of S1 group. Notice: numerous faintly stained hepatocytes in the cortical region.

(X200)

Figures 19&20 (S2): showing decreased staining affinity of total protein in most hepatocytes of the central and portal areas of S2 group, but blood cells inside the hepatic portal vein, walls of bile ducts (bd) acquire increased staining affinity. Notice: moderately to faintly stained total protein in the delaminated epithelial lining of the central vein (CV).

(X200)

Table 1: showing total protein content in the liver tissue of the control and all treated groups of the pregnant rats

Total protein materials	
Experimental groups	Organ
	Liver M ± SD
C	0.85±0.08
S1	0.53±0.06
S2	0.44±0.03*

-Each value represents the mean (M) ± standard deviation (SD).

-* Significant difference from the control at $P \leq 0.05$.

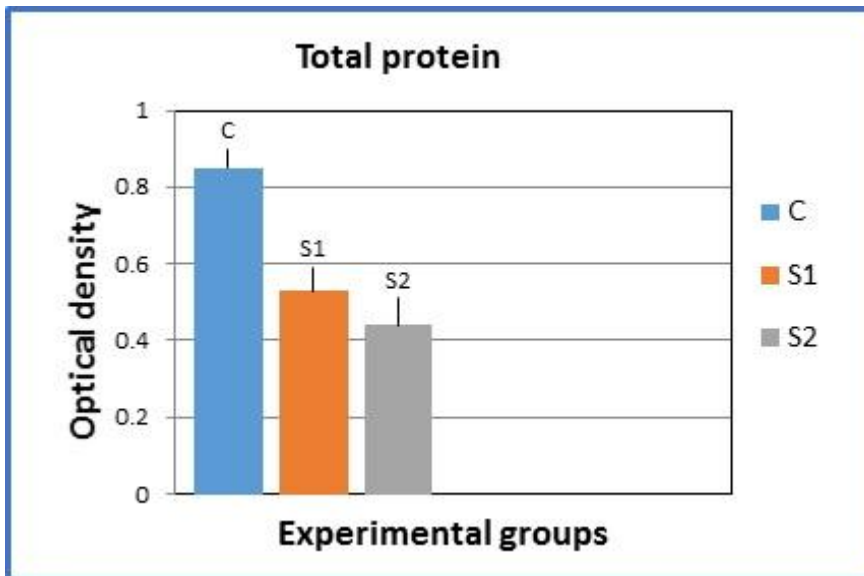
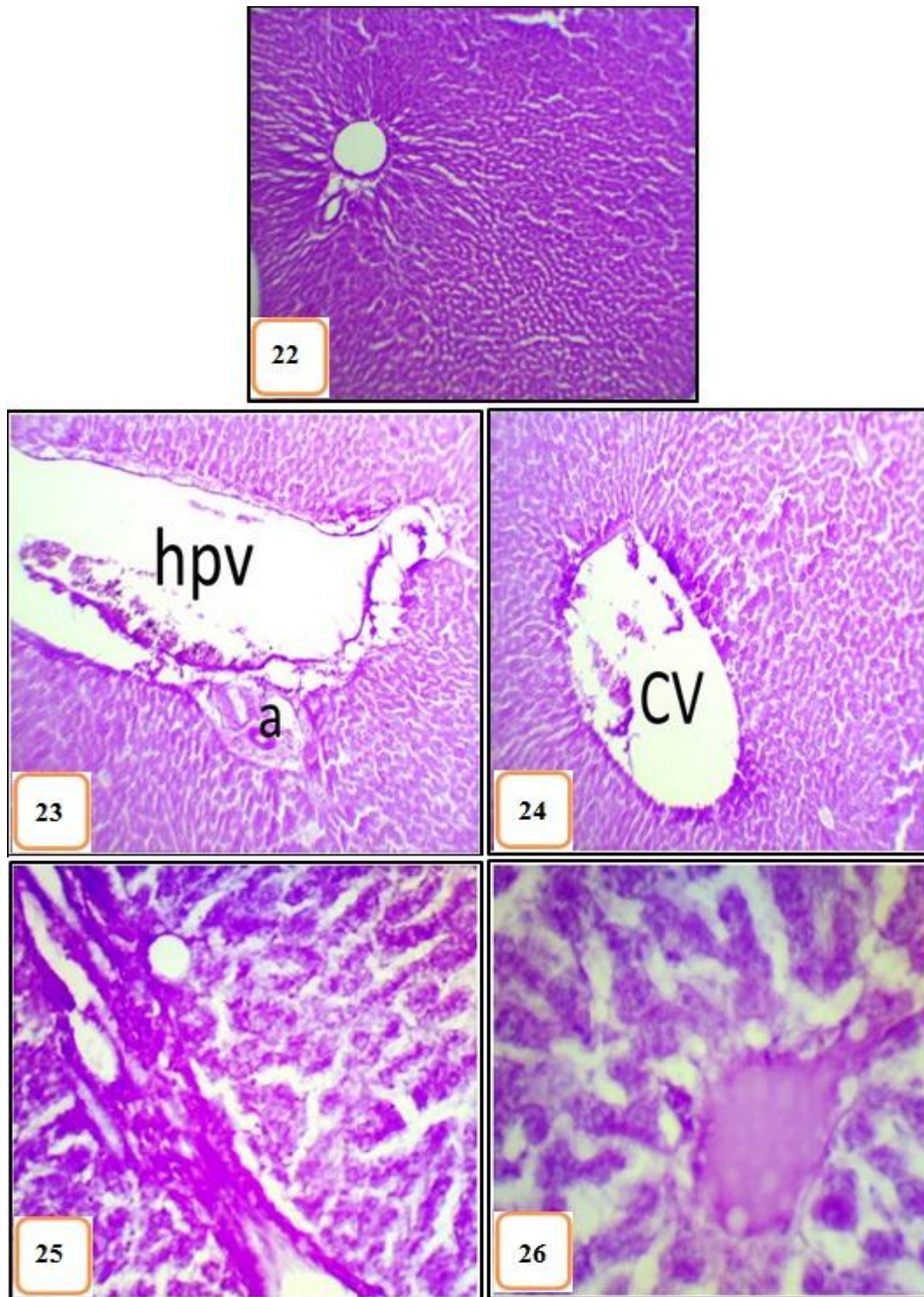


Fig.21: showing mean values of optical density of total protein content relative to the control value.



Figures 22-26: photomicrographs of the liver tissue of the control and treated groups of pregnant rats showing distribution of PAS+ve materials.

Fig.22: showing normal distribution of polysaccharides in the liver tissue of the control pregnant rat.

(X100)

Figures 23&24 (S1): showing reduced staining affinity of PAS+ve materials in the liver tissue of S1 group especially in most hepatocytes of the central and portal areas, but the delaminated epithelial lining of the hepatic portal vein (hpv), the highly thickened arterial wall (a) and damaged blood cells inside the hepatic portal vein (hpv) and the central vein (CV) show increased staining affinity.

(X200)

Figures 25&26 (S2): showing highly depleted PAS+ve materials in most hepatocytes of the liver tissue of S2 group, but walls of the bile ducts, arterial walls, walls of the branches of the hepatic portal veins and the large hemorrhagic area acquire increased staining affinity. **(X 400)**

Table 2: showing PAS+ve materials in the liver tissue of the control and all treated groups of the pregnant rats

PAS+ve materials	
Experimental groups	Organ
	Liver M ± SD
C	0.70±0.06
S1	0.27±0.02*
S2	0.35±0.02*

-Each value represents the mean (M) ± standard deviation (SD).

-* Significant difference from the control at $P \leq 0.05$.

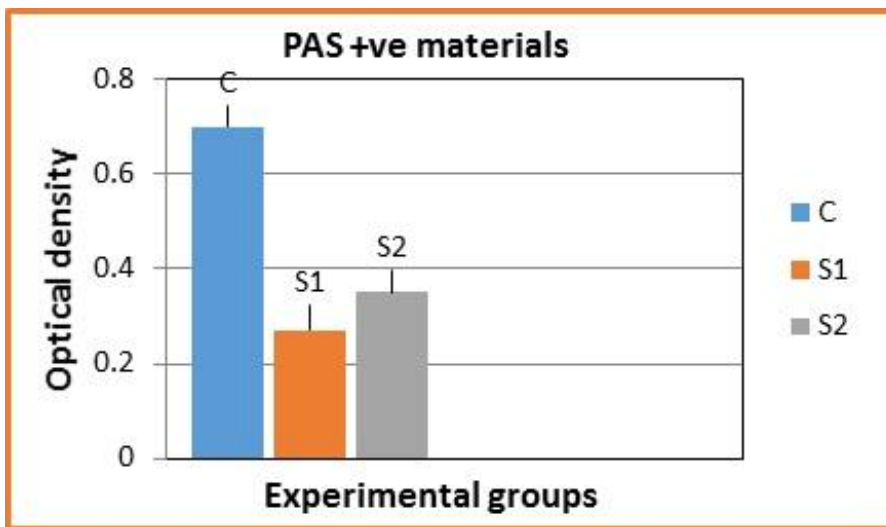
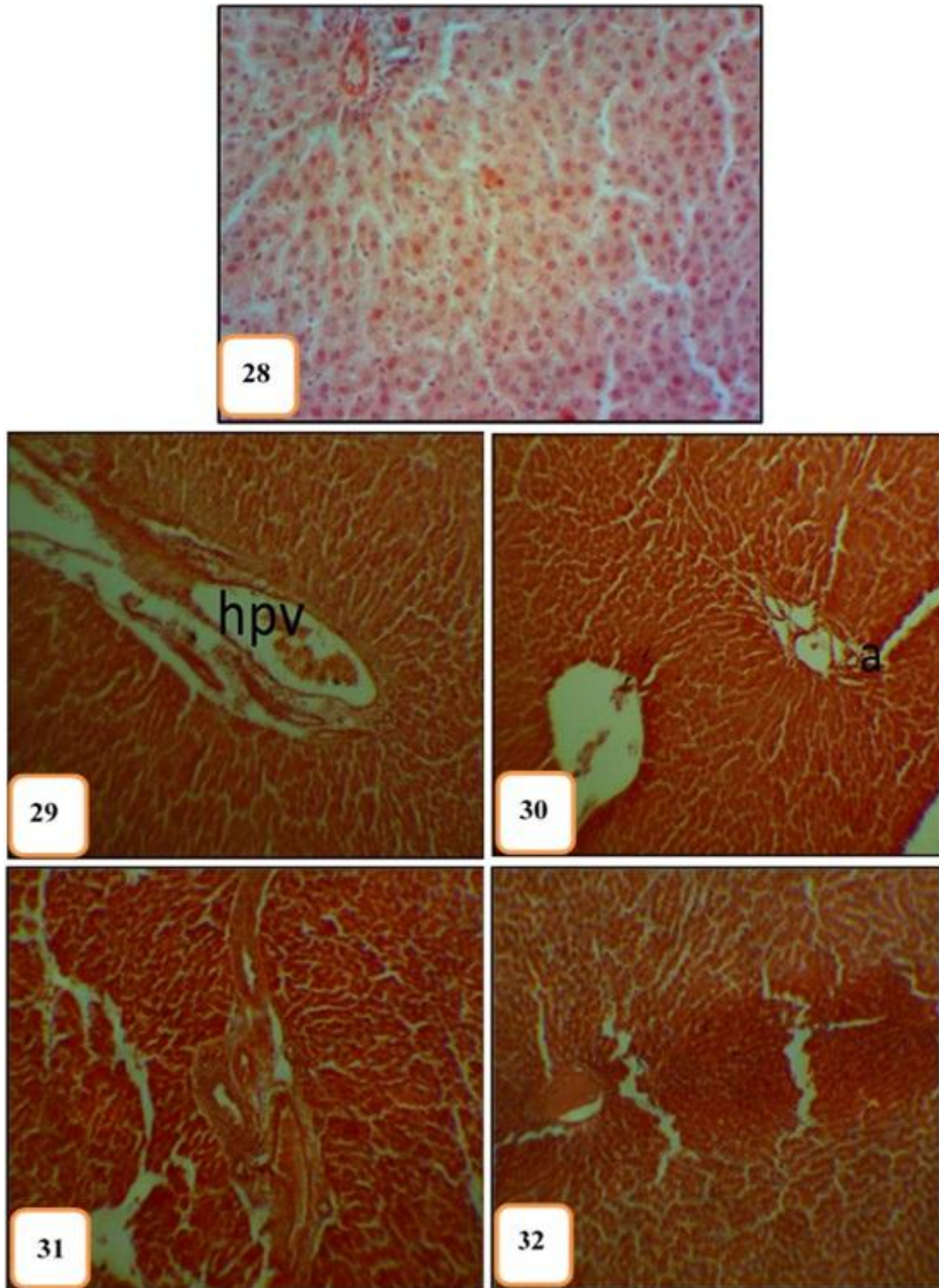


Fig.27: showing mean values of PAS+ve materials relative to the control value.



Figures 28-32: photomicrographs of the liver tissue of the control and treated groups of pregnant rats showing distribution of amyloid- β protein stained with Congo red stain.

Fig.28: showing faintly stained amyloid- β protein in the liver tissue of the control pregnant rat. (X200)

Figures 29&30 (S1): showing increased amyloid deposits in liver tissue of **S1** group especially in the hepatocytes of the cortical region, in the delaminated epithelial lining of the hepatic portal vein (hpv), in the arterial wall (a), in walls of the bile ducts and inside the blood vessels. (X200)

Figures 31&32 (S2): showing deeply stained amyloid deposits in most hepatocytes of the portal and central areas, inside the congested artery, in walls of bile ducts and blood vessels of the liver tissue of **S2** group. **(X200)**

Table 3: showing amyloid-β protein in the liver tissue of the control and all the treated groups of the pregnant

Amyloid – β protein	
Experimental groups	Organ
	Liver M ± SD
C	0.21±0.01
S1	1.00±0.11*
S2	1.16±0.11*

-Each value represents the mean (M) ± standard deviation (SD).

-* Significant difference from the control at $P \leq 0.05$

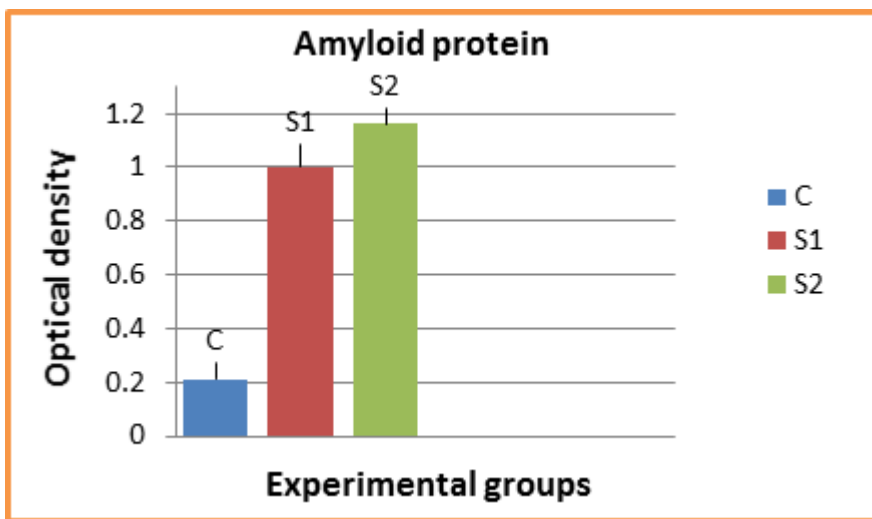
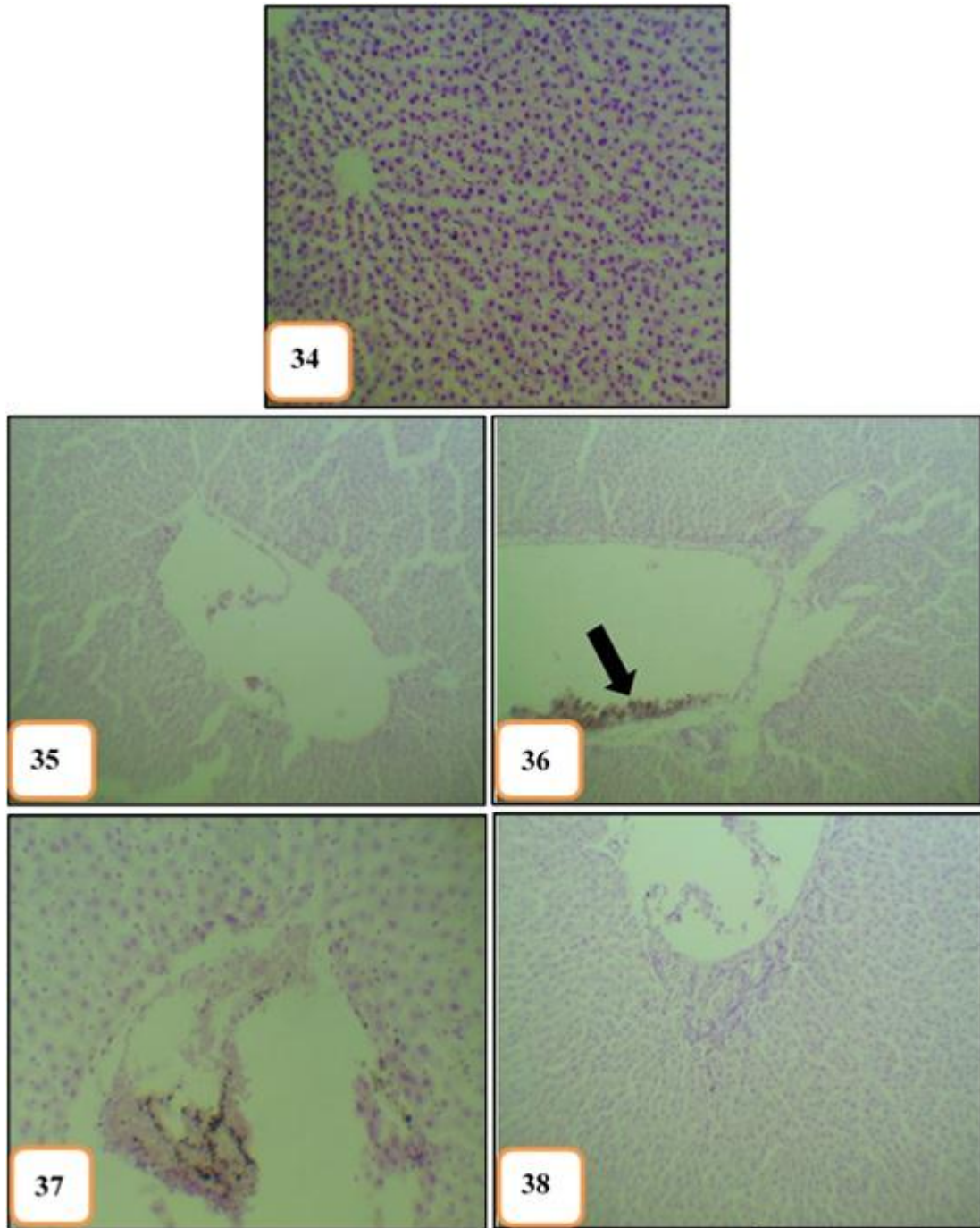


Fig.33: showing mean values of amyloid-β protein relative to the control value.



Figures 34-38: photomicrographs of the liver tissue of the control and treated groups of a pregnant rat stained with Feulgen reaction to detect DNA materials.

Fig. 34: showing moderately stained nuclei of hepatocytes in the liver tissue of a control pregnant rat.

(X200)

Figures 35&36 (S1): showing highly reduced DNA materials in most nuclei of hepatocytes, in the central and portal areas of the liver tissue of S1 group. Notice: lots of darkly stained hemosiderin granules (**➡**).

(X200)

Figures 37&38 (S2): showing decreased DNA materials in most hepatocytes of the central and portal areas of liver tissue of S2 group.

(37 X400 & 38 X250)

Table 4: showing DNA content in the liver tissue of the control and all the treated groups of pregnant rats.

DNA content	
Experimental groups	Organ
	Liver M ± SD
C	0.83±0.03
S1	0.16±0.02*
S2	0.31±0.02*

-Each value represents the mean (M) ± standard deviation (SD).

-* Significant difference from the control at $P \leq 0.05$.

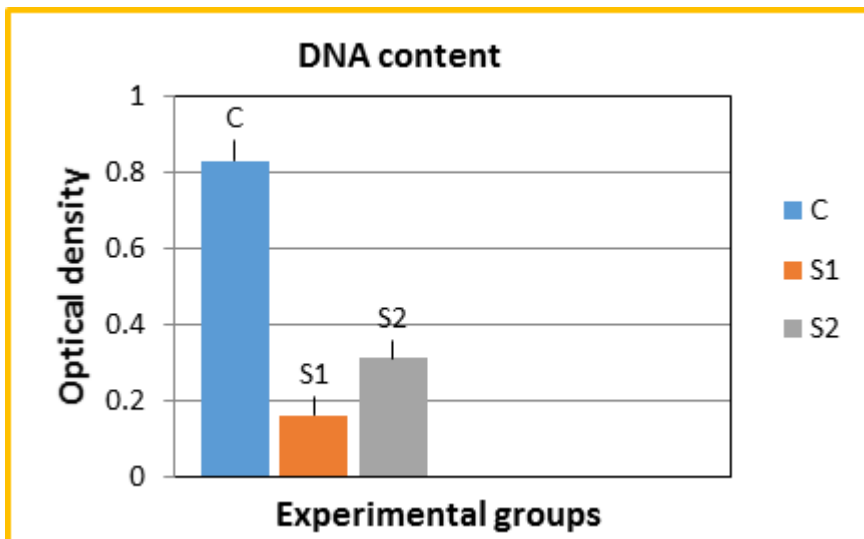


Fig.39: mean values of DNA content relative to the control value.

Results of the fetuses

Fig.40 showed fetal liver tissue of the control group. The central vein was surrounded by hepatocytes and sinusoidal spaces in between the hepatocytes and Kupffer cells were detected. **Fig.41** showed highly dilated and congested central vein which contained hemolysed blood cells, pyknotic nuclei of hepatocytes and with numerous necrotic area of **group S1**. **Fig.42** showed completely hemolysed blood cells in the highly congested central veins and inside the congested sinusoidal spaces with hemosiderin granules in between the hepatocytes. **Fig.43** showed highly dilated sinusoidal spaces, which contained debris of degenerated blood cells and pyknotic nuclei of the megakaryocytes of liver tissue of **group S1**. **Figures 44-47** showed numerous dystrophic changes in the fetal liver

tissue of **group S2**. These changes included: large and small hemorrhagic areas, highly dilated and congested blood vessels, lots of megakaryocytes, numerous degenerated hepatocytes which were replaced by wide necrotic areas. The liver tissue was surrounded by large edematous area.

Fig.48 showed thin bundles of collagen fibers which supported walls of hepatocytes, blood sinusoids and walls of the blood vessel in the fetal liver tissue of a control rat which stained with Mallory's trichrome stain for detection of collagen fibers. **Fig.49** showing highly increased collagen fibers in the dilated central vein and sinusoidal spaces and also in between the hepatocytes of liver tissue of **group S1**. **Figures 50&51** showed increased collagen fibers in the sinusoidal spaces with brightly red stained red blood cells in the highly dilated and congested

blood sinusoidal spaces. Fetal liver tissue of **group S2 (Figures 52-55)** showed highly increased collagen fibers inside and outside the blood vessels, in the necrotic areas and in the megakaryocytes. Notice: brightly red stained blood cells in the numerous hemorrhagic areas and inside the dilated sinusoidal spaces.

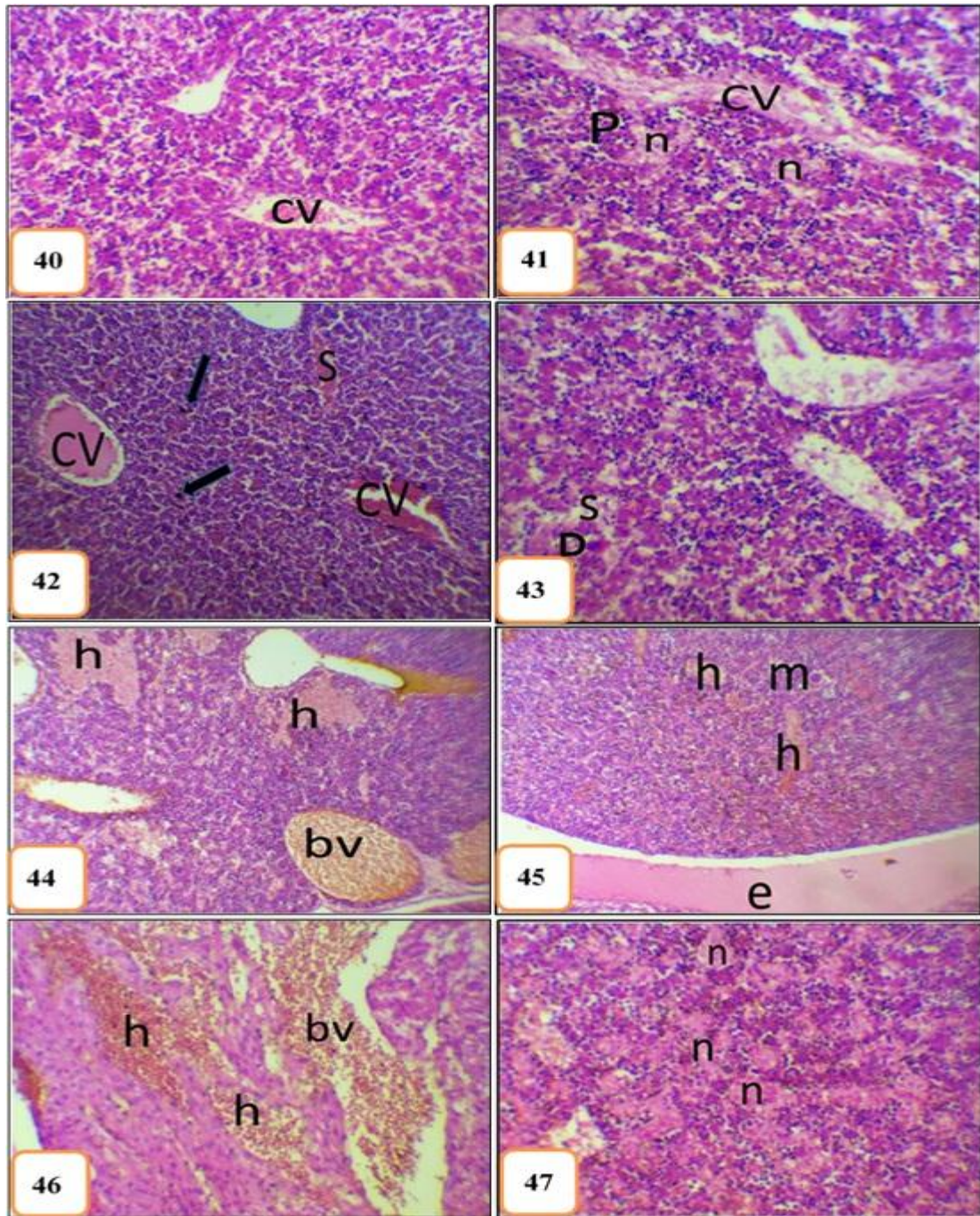
Fig.56 showed moderately stained total protein in the fetal liver tissue of the control group. Liver tissue of **group S1 (Figures 57&58)** showed decreased staining affinity of total protein in the hepatocytes, hemolysed blood cells inside the central vein, the sinusoidal spaces and megakaryocytes. Optical density reached 0.51 ± 0.04 in comparison with the control group (1.08 ± 0.14). Liver tissue of **group S2 Figures 59** showed moderately stained total protein in the hepatocytes, but hemolysed blood cells in the dilated and congested central vein which acquired deep staining affinity. Optical density reached 0.49 ± 0.05 in comparison with the control group (**Table5 and fig.60**).

Fig.61 showed normal distribution of polysaccharides in the fetal liver tissue of the control group. **Figures 62&63** showed moderate staining affinity in most hepatocytes of liver tissue of **S1 group**, increased red blood cells inside the congested blood vessels and sinusoidal spaces and also in the hemorrhagic areas; optical density reached 0.28 ± 0.01 in comparison with the control group (0.14 ± 0.01). **Fig.64** showed moderately stained PAS+ve materials in the hepatocytes of liver tissue of **S2 group** with increased staining affinity in the megakaryocytes. Notice: faintly stained hemolysed blood cells inside the blood

vessels, in the hemorrhagic areas and in the blood sinusoids, but deeply stained hemosiderin granules were observed; optical density reached 0.52 ± 0.05 in comparison with the control group (**Table6 and fig.65**).

Fig.66 showed faintly stained amyloid- β protein (Congo red stain) in the fetal liver tissue of the control group. **Figures 67&68** showed increased staining affinity of amyloid protein in most hepatocytes, blood cells and also in the hemolysed blood cells of the fetal liver tissue of **group S1**; optical density reached 0.96 ± 0.07 in comparison with the control group (0.11 ± 0.01). **Fig.69** showed highly increased amyloid deposits in liver tissue of **group S2** especially in the hepatocytes, blood vessels and in the necrotic areas of the fetal liver tissue; optical density reached 1.03 ± 0.13 in comparison with the control group (**Table7 and fig.70**).

Fig.71 showed moderately stained nuclei of hepatocytes in the fetal liver tissue of a control group stained with Feulgen reaction to detect DNA materials. **Figures 72&73** showed highly reduced staining affinity of DNA materials in most hepatocytes and megakaryocytes of fetal liver tissue of **group S1**. Notice: black stained hemosiderin granules; optical density reached 0.20 ± 0.01 in comparison with the control group (0.30 ± 0.02). **Fig.74** showed poorly to moderately stained DNA materials in nuclei of hepatocytes of the fetal liver tissue of **group S2**. Notice: black stained hemosiderin granules; optical density reached 0.24 ± 0.01 in comparison with the control group (**Table8 and fig.75**).



Figures 40-47: photomicrographs of fetal liver tissue of the control and treated groups (S1&S2) stained with hematoxylin and eosin.

Fig.40: showing fetal liver tissue of the control group. Notice: the central vein (CV) which is surrounded by hepatocytes and sinusoidal spaces. (X200)

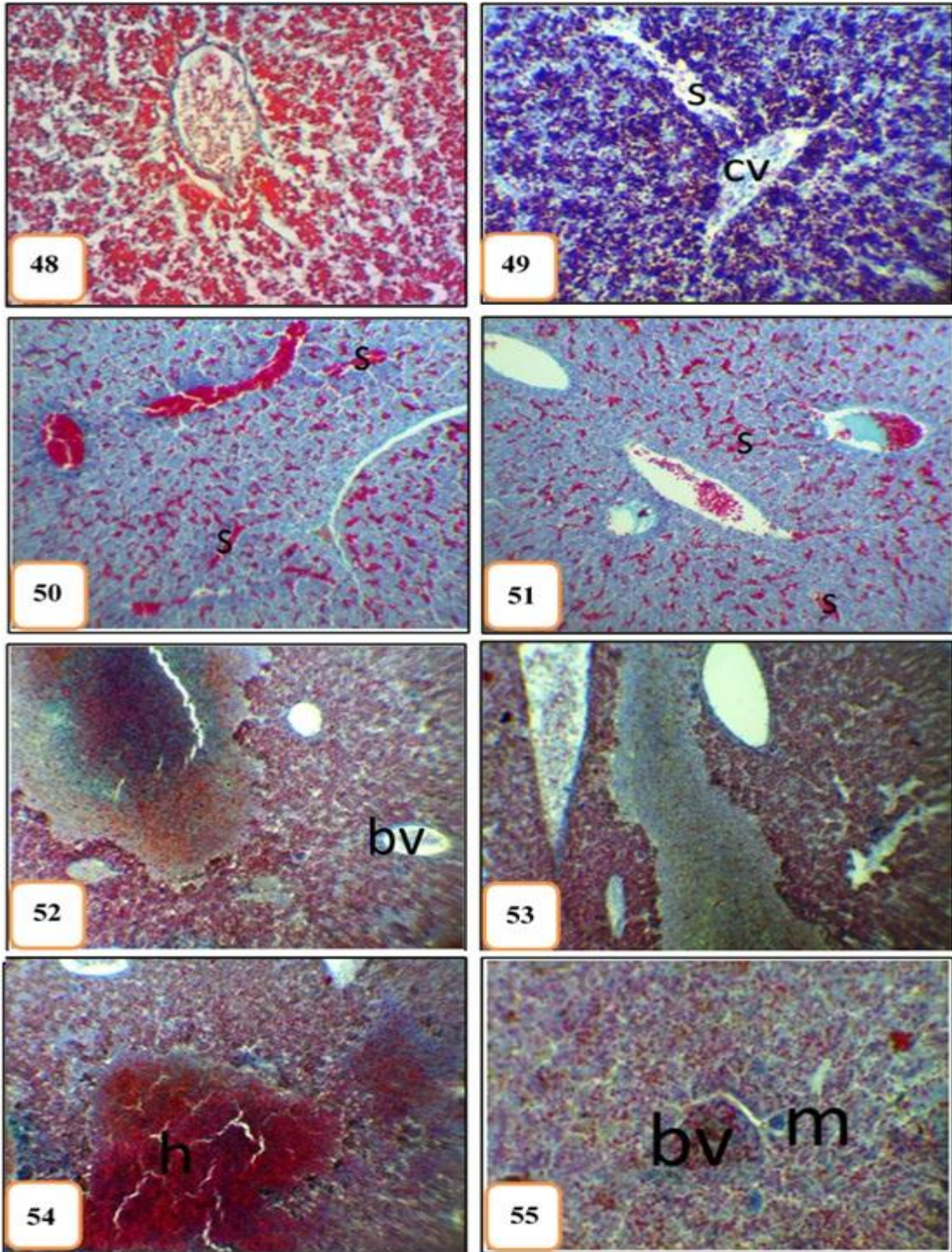
Fig.41 (S1): showing highly dilated and congested central vein (CV) which contains hemolysed blood cells, pyknotic nuclei of hepatocytes (P) and hematopoietic cells with numerous necrotic area (n). (X200)

Fig.42 (S1): showing completely hemolysed blood cells in the highly congested central veins (CV) and inside the congested sinusoidal spaces (S). Notice: hemosiderin granules (➡) in between the hepatocytes. (X250)

Fig.43 (S1): showing highly dilated sinusoidal spaces (S) which contain debris of degenerated blood cells and pyknotic nuclei of the megakaryocytes (P). (X250)

Figures 44-47 (S2): showing numerous dystrophic changes in the fetal liver tissue. These changes include: large and small hemorrhagic areas (h), highly dilated and congested blood vessels (bv), megakaryocytes (m).

The liver tissue is surrounded by large edematous area (e), numerous degenerated hepatocytes which are replaced by wide necrotic areas (n). (44&45 X200 & 46&47 X250)



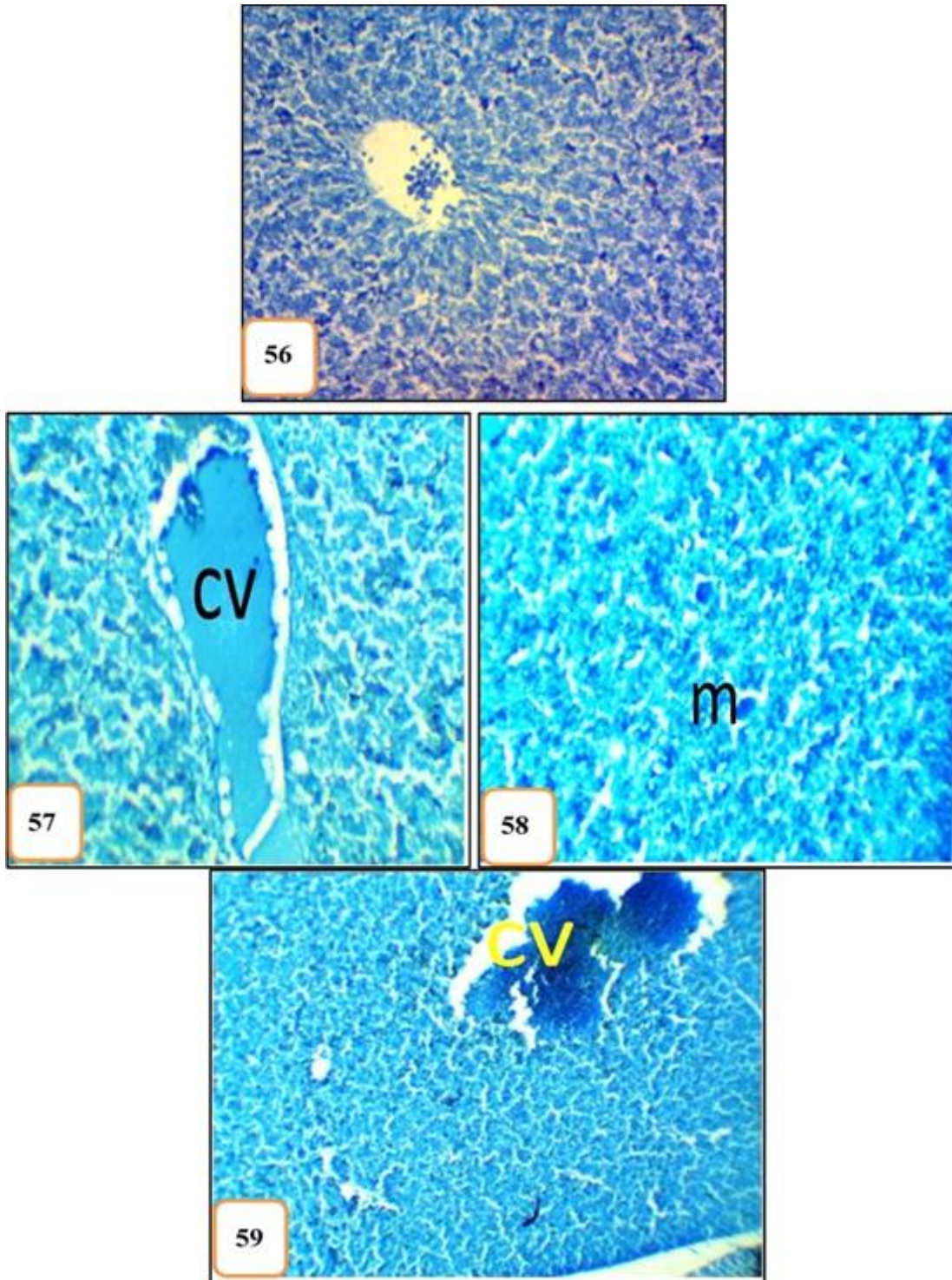
Figures 48-55: photomicrographs of fetal liver tissue of the control and treated groups (S1&S2) stained with Mallory's trichrome stain for detection of collagen fibres.

Fig.48: showing thin bundles of collagen fibers support walls of hepatocytes, blood sinusoids and walls of the blood vessel in the fetal liver tissue of a control rat. (X200)

Fig.49 (S1): showing highly increased collagen fibres in the dilated central vein (CV) and sinusoidal spaces (s) and in between the hepatocytes. (X250)

Figures 50&51 (S1): showing increased collagen fibres in the sinusoidal spaces. Notice: red brightly stained red blood cells in the highly dilated and congested blood sinusoidal spaces (s). (X200)

Figures 52-55 (S2): showing highly increased collagen fibres inside and outside the blood vessels (bv), in the necrotic areas and in the megakaryocytes (m). Notice: red brightly stained blood cells in the numerous hemorrhagic areas (h) and inside the dilated sinusoidal spaces. (X200)



Figures 56-59: photomicrographs of fetal liver tissue of the control and treated groups (S1&S2) showing total protein stained with mercuric bromophenol blue.

Fig.56: showing moderately stained total protein content in the fetal liver tissue of the control group. (X200)

(X200)

Figures 57&58 (S1): showing decreased staining affinity of total protein in the hepatocytes, hemolysed blood cells inside the central vein (CV), the sinusoidal spaces and megakaryocytes (m). (X250)

(X250)

Fig.59 (S2): showing moderately stained total protein in the hepatocytes, but hemolysed blood cells in the dilated and congested central vein (CV) acquire deep staining affinity. **(X200)**

Table 5: showing total protein content in the fetal liver tissue of the control and all treated groups.

Total protein materials	
Experimental groups	Organ
	Liver M ± SD
C	1.08±0.14
S1	0.51±0.04*
S2	0.49±0.05*

-Each value represents the mean (M) ± standard deviation (SD).

-* Significant difference from the control at $P \leq 0.05$.

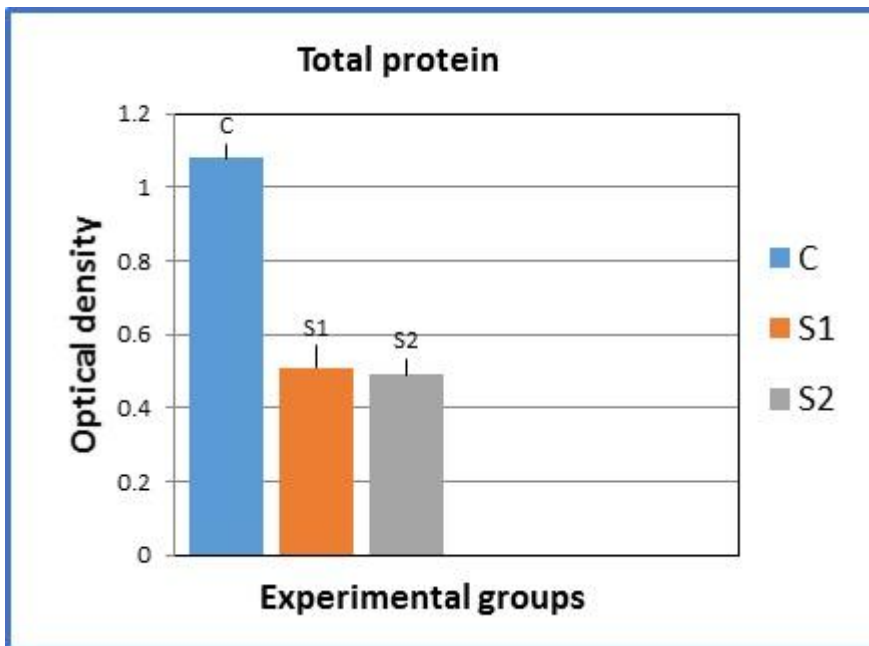
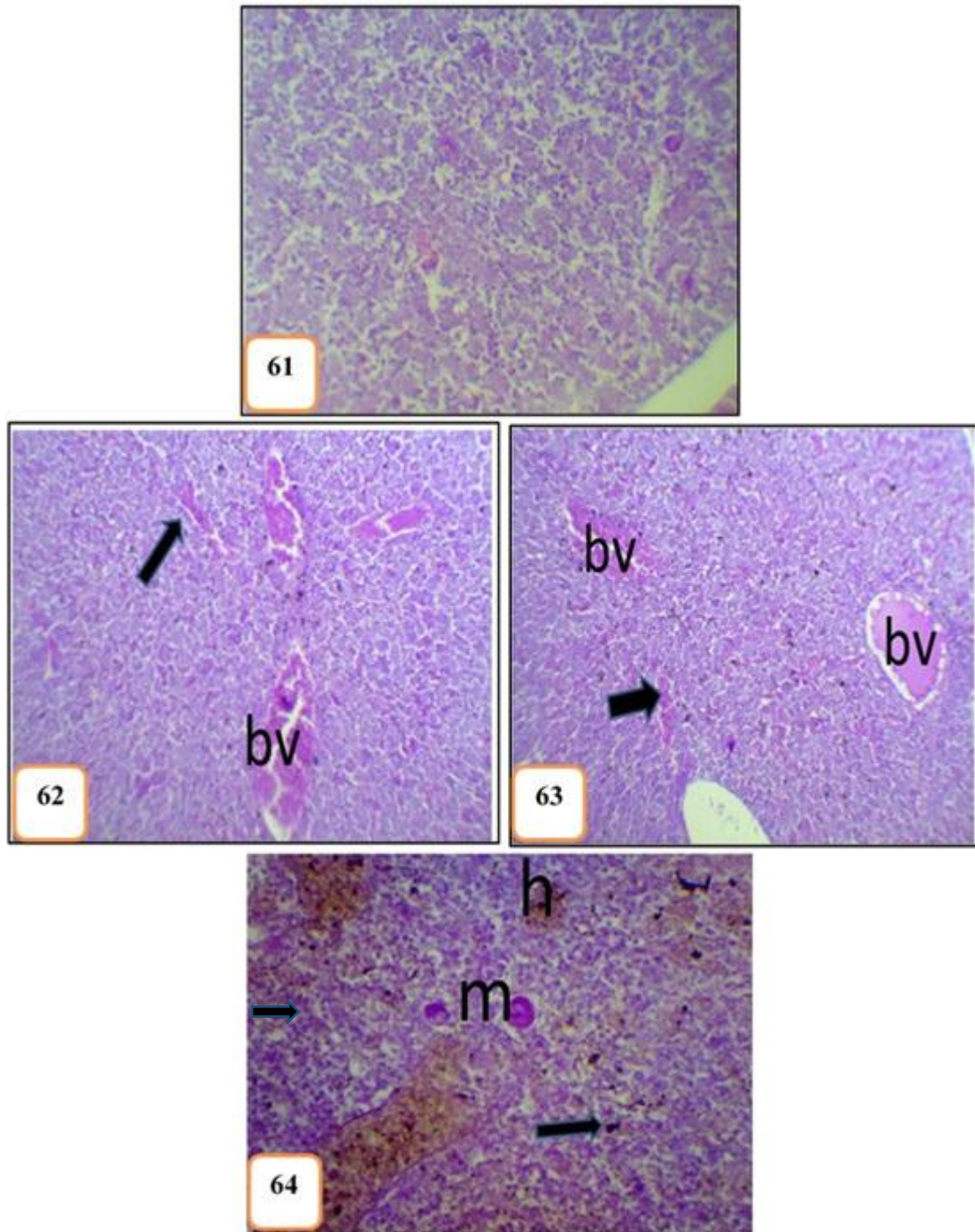


Fig.60: showing mean values of optical density of total protein content relative to the control value.



Figures 61-64: photomicrographs of the fetal liver tissue of the control and treated groups (S1&S2) showing distribution of PAS+ve materials.

Fig.61: showing normal distribution of polysaccharides in the fetal liver tissue of the control group.

(X250)

Figures 62&63 (S1): showing moderate staining affinity in most hepatocytes of S1group, red blood cells inside the congested blood vessels(bv) and sinusoidal spaces and also in the hemorrhagic areas (➡).

(X200)

Fig.64 (S2): showing moderately stained PAS+ve materials in the hepatocytes with increased staining affinity in the megakaryocytes (m). Notice: faintly stained hemolysed blood cells inside the blood vessels, in the hemorrhagic areas (h) and in the blood sinusoids. Notice: deeply stained hemosiderin granules (➡).

(X250)

Table 6: showing PAS+ve materials in the fetal liver tissue of the control and all treated groups.

PAS+ve materials	
Experimental groups	Organ
	Liver M ± SD
C	0.14±0.01
S1	0.28±0.01*
S2	0.52±0.05*

-Each value represents the mean (M) ± standard deviation (SD).

-* Significant difference from the control at $P \leq 0.05$.

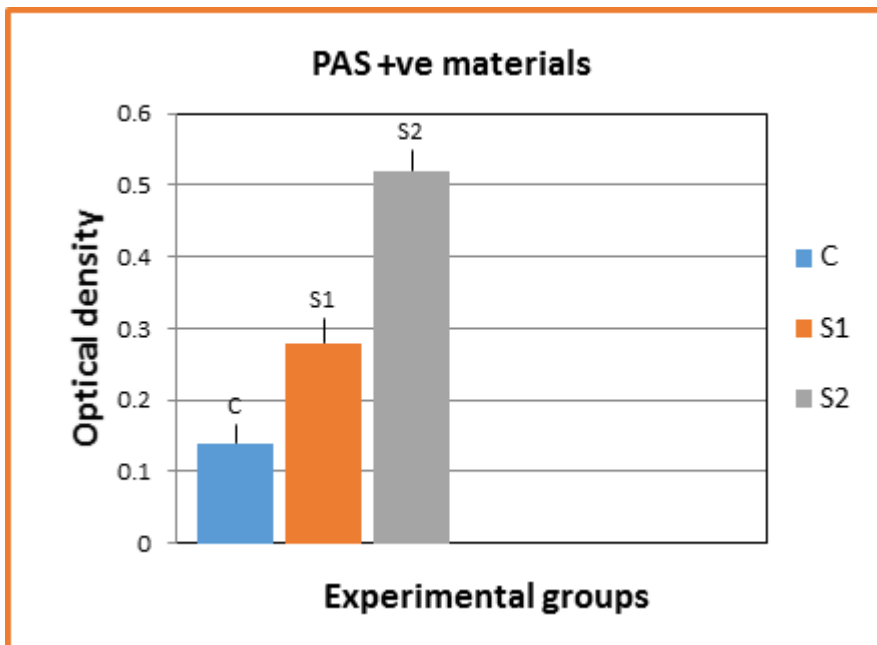
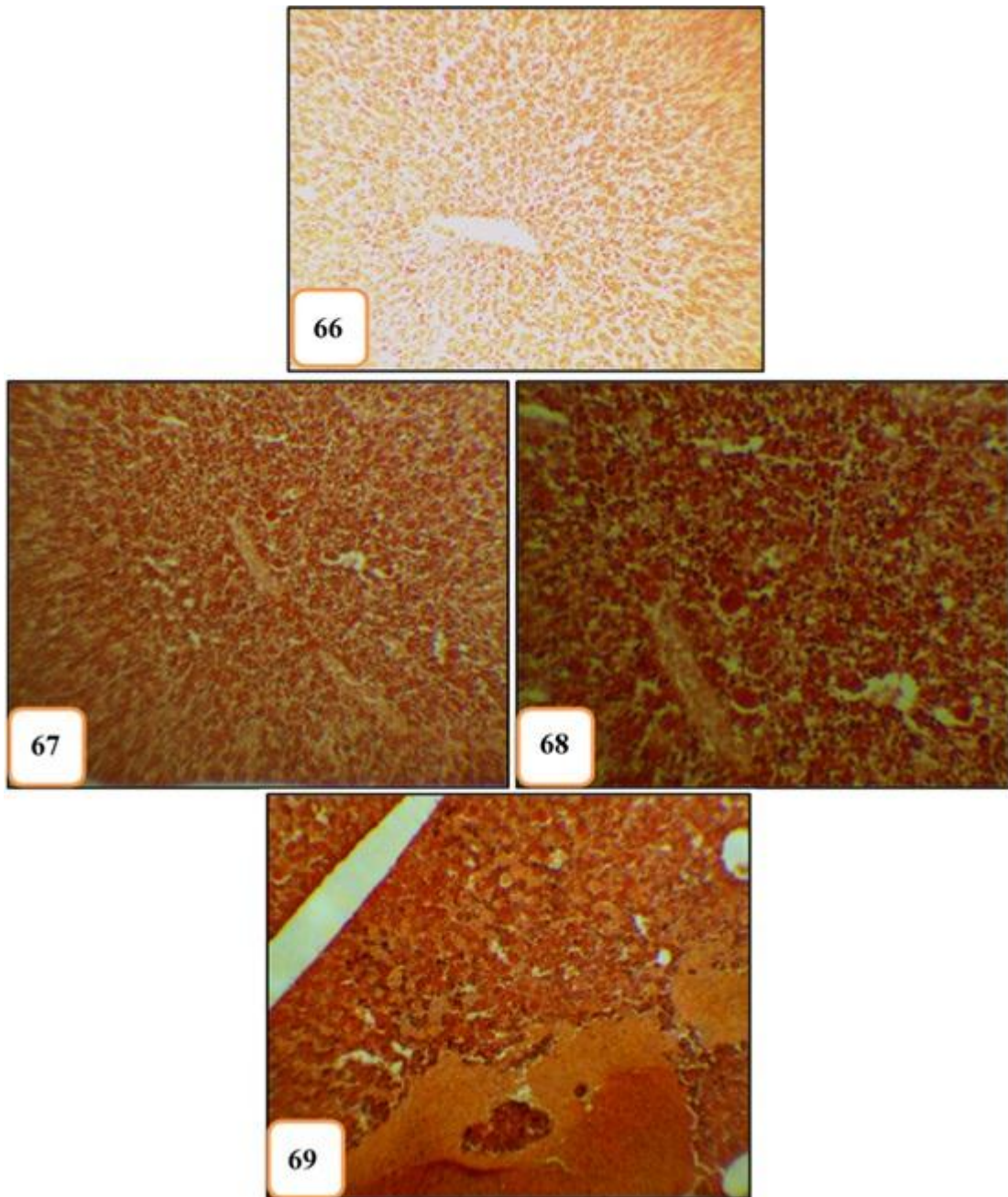


Fig.65: showing mean values of PAS+ve materials relative to the control value.



Figures 66-69: photomicrographs of fetal liver tissue of the control and treated groups (S1&S2) showing distribution of amyloid- β protein stained with Congo red stain.

Fig.66: showing faintly stained amyloid- β protein in fetal liver tissue of the control group.

(X200)

Figures 67&68 (S1): showing increased staining affinity of amyloid protein in most hepatocytes, blood cells and also in the hemolysed blood cells of the fetal liver tissue of S1 group.

(67X200 & 68X250)

Fig.69 (S2): showing highly increased amyloid deposits in the hepatocytes, blood vessels and in the necrotic areas of the fetal liver tissue of S2 group.

(X200)

Table 7: showing amyloid-β protein in fetal liver tissue of the control and all the treated groups.

Amyloid – β protein	
Experimental groups	Organ
	Liver M ± SD
C	0.11±0.01
S1	0.96±0.07*
S2	1.03±0.13*

-Each value represents the mean (M) ± standard deviation (SD).

-* Significant difference from the control at $P \leq 0.05$.

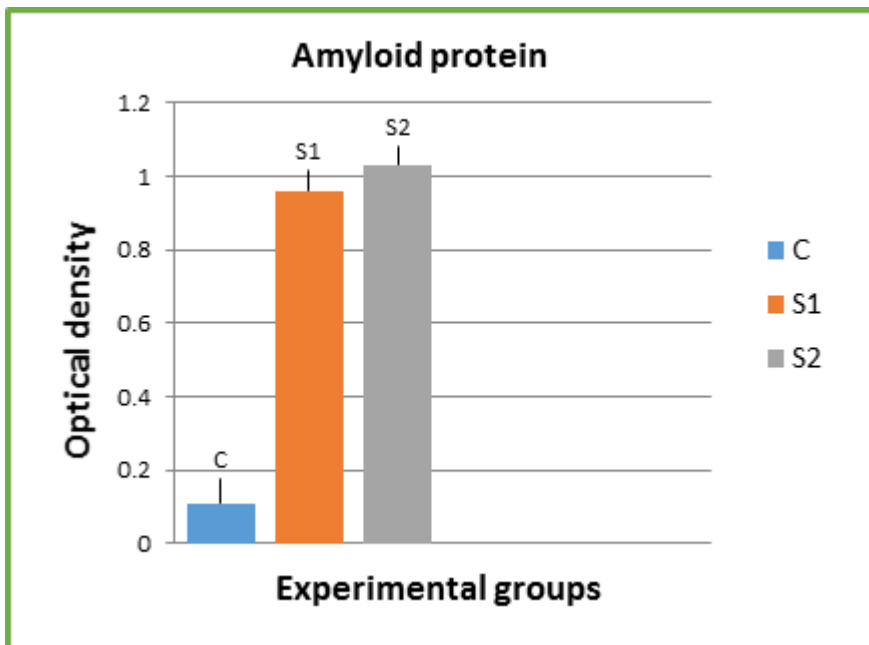
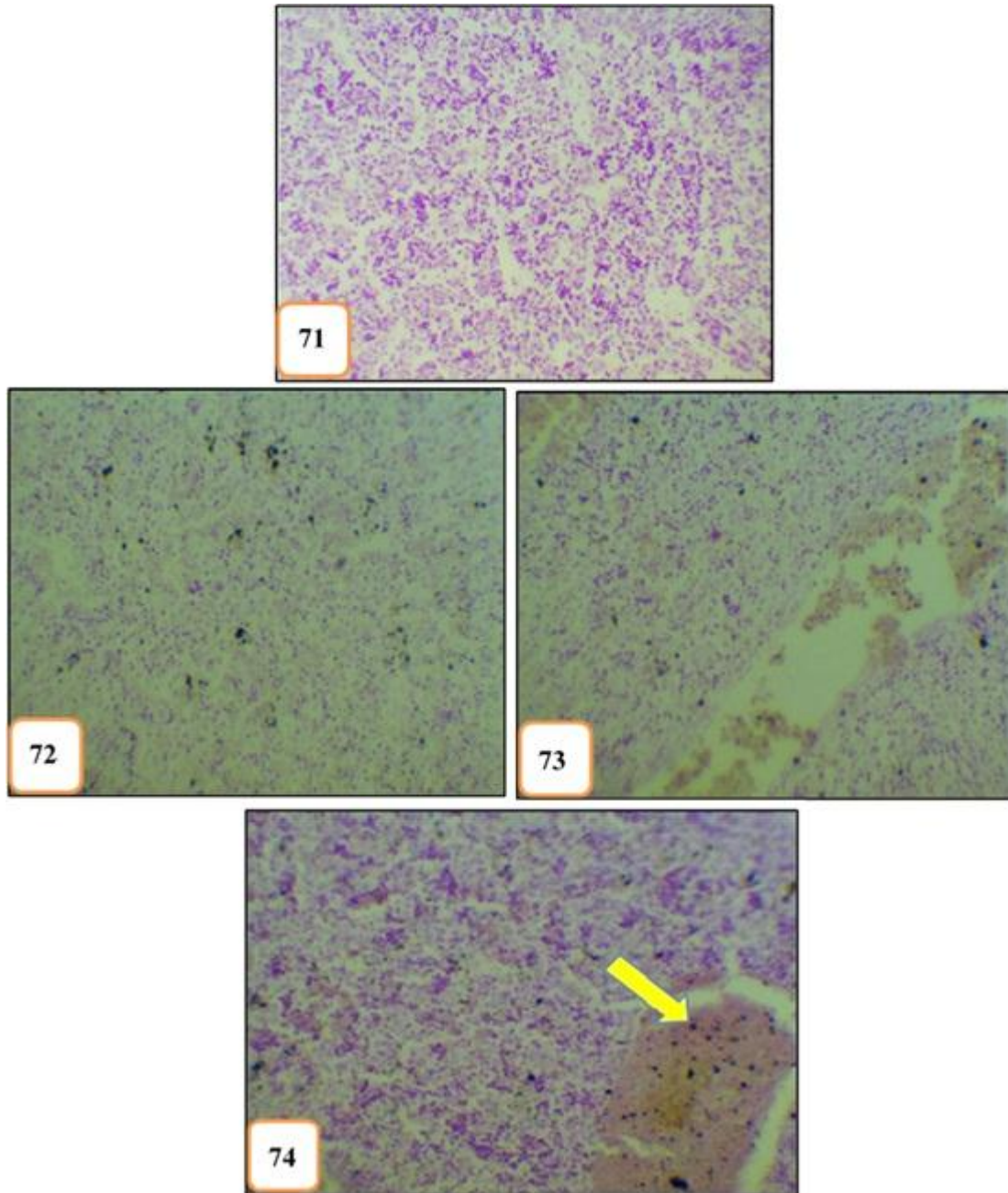


Fig.70: showing mean values of amyloid-β protein relative to the control value.



Figures 71-74: photomicrographs of fetal liver tissue of the control and treated groups (**S1&S2**) stained with Feulgen reaction to detect DNA materials.

Fig.71: showing moderately stained nuclei of hepatocytes in the fetal liver tissue of a control group.

(X200)

Figures 72&73 (S1): showing highly reduced staining affinity of DNA materials in most hepatocytes and megakaryocytes of fetal liver tissue of **S1**group. Notice: black stained hemosiderin granules.

(X250)

Fig.7 (S2): showing poorly to moderately stained DNA materials in nuclei of hepatocytes of the fetal liver tissue of **S2** group. Notice: black stained hemosiderin granules (**➡**).

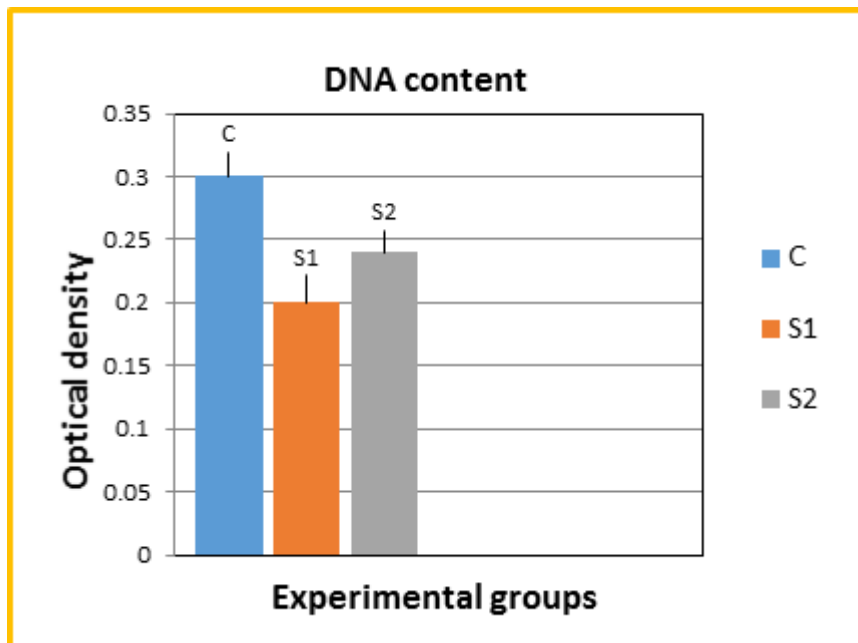
(X250)

Table 8: showing DNA content in fetal liver tissue of the control and all the treated groups.

DNA content	
Experimental groups	Organ
	Liver M ± SD
C	0.30±0.02
S1	0.20±0.01*
S2	0.24±0.01*

-Each value represents the mean (M) ± standard deviation (SD).

-* Significant difference from the control at $P \leq 0.05$.

**Fig.75:** Mean values of DNA content relative to the control value.

DISCUSSION

Liver is a very important organ for healthy and life of mammals. Reason for selection of liver tissue for this study is its sensitivity to waste products. The most important features of the pathologic changes were increased bilirubin, ALAT and ASAT enzymes activities in the serum. During cell injury, because of higher permeability of hepatocyte membrane, these enzymes (ALAT and ASAT) penetrate the sinusoids and then enter the peripheral blood and increase levels of such enzymes⁽²⁵⁾. In animals, carisoprodol produces muscle relaxation by blocking interneuronal activity in the descending reticular fibres and

spinal cord; however it is unknown if this mechanism of action is also present in humans⁽²⁶⁾. Rapid gastrointestinal absorption results in peak carisoprodol plasma concentrations of 4 mg/mL to 7 mg/mL within 2–4 h and onset of action is within 30 min of ingestion. Carisoprodol undergoes dealkylation and oxidation in the liver. Hydroxymeprobamate, meprobamate and hydroxycarisoprodol were the major metabolites identified in the blood and urine; trace quantities of unchanged carisoprodol were also detected in the urine^(27, 28).

In the present study, treatment of pregnant rats with carisoprodol caused numerous

degenerative changes in liver tissue of the pregnant rats of group S1. These changes included: highly congested and dilated central veins and blood sinusoids, formation of hemosiderin granules and hemolysed blood cells inside the hepatic portal veins, highly thickened arterial walls in the portal areas, highly distorted portal areas, some hepatocytes were vacuolated and contained pyknotic or karyolytic nuclei. Also, liver tissue of pregnant rats of group S2 showed many dystrophic changes. These changes included: delaminated endothelial lining of the central veins, vacuolated hepatocytes with pyknotic nuclei, highly elongated and distorted walls of the bile ducts, large hemorrhagic areas and numerous fibroblasts in the portal areas. Examination of the fetal liver tissue of group S1 showed highly dilated and congested central veins which contained hemolysed blood cells, pyknotic nuclei of hepatocytes with numerous necrotic area. Completely hemolysed blood cells were detected in the highly congested central veins and inside the congested sinusoidal spaces with hemosiderin granules in between the hepatocytes. Highly dilated sinusoidal spaces, which contained debris of degenerated blood cells and pyknotic nuclei of the megakaryocytes were realized. In the second group (S2), liver sections showed numerous dystrophic changes. These changes included: large and small hemorrhagic areas, highly dilated and congested blood vessels, lots of megakaryocytes numerous degenerated hepatocytes which were replaced by wide necrotic areas. The liver tissue was surrounded by large edematous area. **Chan** ⁽²⁹⁾ reported that liver weights were significantly greater in males administered 300 mg/kg of carisoprodol in corn oil or greater and in females administered 150 mg/kg of carisoprodol in corn oil or greater as compared to the control group. Also, carisoprodol in 0.5% methylcellulose induced increases in relative liver weights of males and females mice and also induced increases in the incidences of centrilobular hypertrophy of hepatocytes in the liver of males of all dosed groups and in females administered 1,200 or 1,600 mg/kg. This lesion was characterized by cells with slightly increased amounts of cytoplasm and increased eosinophilic staining affinity. The differences in histopathology findings between mice treated with carisoprodol in corn oil and in 0.5% methylcellulose were probably due to the greater availability of carisoprodol administered in 0.5% methylcellulose. The previous study also showed that carisoprodol treatment clearly increased

chromosomal aberrations in cultured Chinese hamster ovary cells. The increases in liver weights were probably due to induction of cytochrome P450 enzymes ⁽³⁰⁻³²⁾. The previous changes in DNA materials are in agreement with results of the present study; since numerous degenerative changes were detected in nuclei of fetal and maternal liver tissue.

The results of the present study are supported by results of **Van der Kleijn** ⁽³³⁾ who showed that the radiolabeled carisoprodol was taken up by the central nervous system of mice within 40 seconds after intravenous injections of it. The injected carisoprodol was distributed throughout the body within 10 minutes. The highest concentrations were found in the liver, myocardium, pituitary gland and adrenal cortex followed by the blood, lungs and skeletal muscles. Radioactivity was uniformly distributed throughout the fetuses of pregnant mice 15 minutes after the dose was administered. Carisoprodol is biotransformed by the cytochrome P450 drug metabolizing system in the liver ⁽³⁴⁾. Doses of 200 mg/kg carisoprodol to male Wistar rats or 180 mg/kg carisoprodol to Sprague-Dawley female rats caused increases in the hepatic enzymes of the microsomal NADPH-electron transport chain in the male rats, no increases in the liver weights were observed ^(30,32). Induction of the microsomal drug metabolizing enzymes increased carisoprodol metabolism and shortened the duration of paralysis induced by carisoprodol; this induction of metabolizing enzymes may be related to the development of tolerance to carisoprodol with chronic exposure ⁽³¹⁾.

Carisoprodol is excreted in breast milk at concentrations two to four times that in maternal plasma ⁽³⁴⁾. Additionally, the carisoprodol metabolite meprobamate is associated with an increased risk of congenital malformations during the first trimester of pregnancy ⁽³⁵⁾. These results are in agreement with our results since fetal tissue of both groups (S1&S2) were highly affected than maternal liver tissue. Increased risk of developing concentration-dependent side effects even at normal therapeutic doses of carisoprodol were determined by **Dalen et al.** ⁽²⁸⁾.

In the present study highly increased collagen fibres were detected in liver tissue of pregnant rats of group S1 and S2 especially in walls of the bile ducts, blood vessels, hepatocytes and in the distorted portal areas with brightly red stained hemorrhagic areas and aggregated RBCs in the congested blood sinusoids. Also, highly

increased collagen fibres were detected in the dilated central veins and sinusoidal spaces and also in between the hepatocytes of fetal liver tissue of group S1. While, fetal liver tissue of group S2 showed highly increased collagen fibres inside and outside the blood vessels, in the necrotic areas and in the megakaryocytes. **Hassan *et al.***⁽³⁶⁾ reported that increased collagen fibres may lead to increase the defense reaction against toxic materials. According to **Guler *et al.***⁽³⁷⁾ increased collagen deposition may be attributed to oxidative stress that stimulates the expression of genes involved in collagen biosynthesis. Increased superoxide anion formation by inhibition of superoxide dismutase (antioxidant enzyme) stimulates collagen production and this indicated a vital role of superoxide dismutase and the generated reactive oxygen species in collagen accumulation⁽³⁸⁾.

Results of the present study showed decreased total protein content in liver tissue of pregnant rats of groups S1. Also, reduced total protein was detected in liver tissue of group S2, but increased staining affinity was realized in blood cells inside the congested hepatic portal vein and walls of the bile ducts. Also, fetal liver tissue of group S1 showed decreased staining affinity of total protein content in the hepatocytes, hemolysed blood cells inside the central vein, the sinusoidal spaces and megakaryocytes in comparison with the control group. Liver tissue of group S2 showed moderately stained total protein in the hepatocytes, but hemolysed blood cells in the dilated and congested central vein acquired deep staining affinity. Proteins are mainly involved in the architecture of the cell⁽³⁹⁾. Protein is associated with glucose control, insulin regulation, muscle building and regulation or increased metabolism⁽⁴⁰⁾. **Al Gahtani**⁽⁴¹⁾ reported that vacuolation and degeneration led to decreased protein content in the different tissues. **Abuo El Naga and Abd Rabou**⁽⁴²⁾ stated that decreased protein content may be due to ruptured cellular organoids or to decreased polyribosomes. **Abdel-meguid *et al.***⁽⁴³⁾ stated that the decrease in protein could be attributed to the disruption of lysosomal membranes under the effects of various toxicants; thus leading to the liberation of their hydrolytic enzymes in the cytoplasm. Additionally, the presence of hydrolytic enzymes may cause lysis and dissolution of the target material within the cytoplasm.

In the present study, livers of pregnant rats of **S1** group exhibited a significant decrease in PAS positive materials compared to the control

group. Also, highly depleted PAS+ve materials were realized in most hepatocytes of the liver tissue of group S2 in comparison with the control group. Moderately stained PAS+ve materials were observed in most hepatocytes of the fetal liver tissue of S1 and S2 group, increased red blood cells inside the congested blood vessels and sinusoidal spaces and also in the hemorrhagic areas, but increased PAS+ve materials were observed in megakaryocytes. The decrease in carbohydrate contents in the current work may be attributed to increased stress on the organs which leading to consuming high energy in attempt to light or equalize the pressure exerted upon them. It may also be due to the release of hydrolytic enzymes from ruptured lysosomes under the effects of toxic agents. This opinion is supported by the work of **Sakr and Okdah**⁽⁴⁴⁾ and **Farrag and Shalby**⁽⁴⁵⁾.

The current study recorded a significant increase in the amyloid- β deposits in maternal liver tissue of S1 group especially in hepatocytes of the cortical region, in the delaminated epithelial lining of the hepatic portal veins, in the arterial walls, in walls of the bile ducts and inside the blood vessels. Also, deeply stained amyloid deposits were observed in most hepatocytes of the portal and central areas, inside the congested artery, in walls of the bile ducts and blood vessels of the liver tissue of group S2 in comparison with the control group. Highly increased staining affinity of amyloid protein was observed in most hepatocytes, blood cells, necrotic areas and also in the hemolysed blood cells of the fetal liver tissue of group S1 and S2. Amyloids are insoluble fibrous protein aggregates sharing specific structural traits. They are insoluble and arise from at least 18 inappropriately folded versions of proteins and polypeptides present naturally in the body⁽⁴⁶⁾. These misfolded structures alter their proper configuration such that they erroneously interact with one another or other cell components forming insoluble fibrils. They have been associated with the pathology of more than 20 serious human diseases since abnormal accumulation of amyloid fibrils in organs may lead to amyloidosis and may play a role in various neurodegenerative disorders⁽⁴⁷⁾. **Kadowaki *et al.***⁽⁴⁸⁾ showed that amyloid deposition is associated with mitochondrial dysfunction and resulting generation of reactive oxygen species (ROS), which can initiate a signaling pathway leading to apoptosis.

The current results showed highly reduced DNA materials in most nuclei of

hepatocytes, in the central and portal areas in the liver tissue of pregnant rats of group S1 and S2. Also, decreased DNA materials were realized in most hepatocytes and megakaryocytes of fetal liver tissue of group S1 and S2. The decrease in both DNA and total protein in the current work may be attributed to arrested metabolism or to use it to build up new cells or enzymes to reduce the stress and also disruption of lysosomal membranes under the effect of various toxicants leading to liberating of their hydrolytic enzymes in the cytoplasm and resulted in marked lysis and dissolution of the target materials⁽⁴⁹⁾.

REFERENCES

- 1-Pattanayak RD, Ambekar A, Chatterjee B and Ray R (2017):** Substitution of alcohol with carisoprodol: a case for concern. *Indian J. Med. Sci.*, 69(1): 55-56.
- 2-Reeves RR and Burke RS (2010):** Carisoprodol: abuse potential and withdrawal syndrome. *Curr. Drug Abuse Rev.*, 3(1): 33-38.
- 3-Witenko C, Moorman-Li R, Motycka C, Duane K, Hincapie-Castillo J, Leonard P and Valaer C (2014):** Considerations for the appropriate use of skeletal muscle relaxants for the management of acute low back pain. *Phar. Thera.*, 39(6): 427-435.
- 4-Reeves RR and Parker JD (2003):** Somatic dysfunction during carisoprodol cessation: evidence for a carisoprodol withdrawal syndrome. *JAOA.*, 103: 75-80.
- 5-Hoiseth G, Bramness JG, Christophersen AS and Morlan J (2007):** Carisoprodol intoxications: a retrospective study of forensic autopsy material from 1992–2003. *Inter. J. Legal Med.*, 121: 403–409.
- 6-Robertson M and Marinetti L (2003):** Carisoprodol—effects on human performance and behavior. *Forensic Sci. Rev.*, 15: 1-9.
- 7-Gatch MB, Nguyen JD, Carbonaro T and Forster MJ (2012):** Carisoprodol tolerance and precipitated withdrawal. *Drug Alcohol Dependence*, 123(1): 29-34.
- 8-Kumar M and Dillon GH (2016):** Assessment of direct gating and allosteric modulatory effects of meprobamate in recombinant GABA A receptors. *European J. Pharmacol.*, 775: 149-158.
- 9-Bramness JG, Buajordet I and Skurtveit S (2008):** The role of pharmaco-epidemiological studies in the market withdrawal of carisoprodol (Somadril) in Europe. *Norsk. Epidemiologi*, 18(2): 167-172
- 10-Hoiseth G, Karinen R, Sorlid HK and Bramness JG (2009):** The effect of scheduling and withdrawal of carisoprodol on prevalence of intoxications with the drugs. *Basic Clin. Pharmacol. Toxicol.*, 105(5): 345-349.
- 11-McIntyre IM, Sherrard J and Lucas J (2012):** Postmortem carisoprodol and meprobamate concentrations in blood and liver: lack of significant redistribution. *J. Anal. Toxicol.*, 36(3): 177-181.
- 12-Bernal W, Auzinger G, Dhawan A and Wendon J (2010):** Acute liver failure. *The Lancet*, 376: 190-201.
- 13-Reuben A, Koch DG and Lee WM (2010):** Drug-induced acute liver failure: results of a multicenter, a prospective study. *Hepatology*, 52(6): 2065-2076.
- 14-Jain S, Srivastava AS, Verma RP and Maggu G (2017):** Caffeine addiction: Need for awareness and research and regulatory measures. *Asian J. Psychiatry*, 1028: 1-3.
- 15-Lara DR (2010):** Caffeine, mental health, and psychiatric disorders. *J. Alzhe. Dis.*, 20(S1): 239-248.
- 16-Ballet F (2015):** Preventing drug-induced liver injury: how useful are animal models? *Diges. Dis.*, 33(4): 477-485.
- 17-Decker CW, Casian JG, Nguyen KT, Horton LA, Rao MP, Silkwood KH and Han D (2017):** The critical role of mitochondria in drug-induced liver injury. In *molecules, system and signaling in liver injury*. Springer Cham., (8): 159-181.
- 18-Paget GE and Barnes JM (1964):** Interspecies dosage conversion scheme in evaluation of results and quantitative application in different species. In: *Evaluation of Drug Activities*. Laurence D R and Bacharach A L (Eds.). Academic Press, London and USA. pp: 160-162.
- 19-Bancroft J and Gamble M (2002):** Theory and Practice of Histology Techniques. 5th ed. Churchill Livingstone, London. pp: 150-152.
- 20-Mazia D, Brewer PA and Alfert M (1953):** The cytochemical staining and measurement of protein with mercuric bromophenol blue. *Biol. Bull.*, 104(1): 57-67.
- 21-Carleton HM, Drury RAB and Wallington EA (1980):** Carleton's histological technique. 4th ed., Oxford Univ. Press, New York, USA. Pp520.
- 22-Pearse A G (1985):** Histochemistry, Theoretical and Applied. Analytical Technology, 4th ed., vol. 2. Churchill Livingstone, London. Pp.594.
- 23-Valle S (1986):** Special stains in microwave oven. *J. Histotechnol.*, 9(4): 237-239.
- 24-Jaeger TF (2008):** Categorical data analysis: Away from ANOVAs (transformation or not) and towards logit mixed models. *J. Mem. Langu.*, 59(4): 434-446.
- 25-Muriel P (2009):** Role of free radicals in liver diseases. *Hepatol. Int.*, 3(4): 526–536.
- 26-Inoue Y (2002):** Medical economics—Hepatitis C virus infection and cost-effectiveness of Interferon therapy. *Hepato. Res.*, 24: 57-67.
- 27-Littrell RA, Hayes LR and Stillner V (1993):** Carisoprodol (Soma), a new and cautious perspective on an old agent. *South Med. J.*, 86(7): 753-756.
- 28-Dalen P, Alvan G, Wakelkamp M and Olsen H (1996):** Formation of meprobamate from carisoprodol is catalyzed by CYP2C19. *Pharmacogenetics*, 6(5): 387-394.
- 29-Chan PC (2000):** NTP toxicity studies of carisoprodol (CAS No.78-44-4) administered by gavage to F344/N rats and B6C3F1 mice. *Toxic. Rep. Ser.*, (56): 1-G14.

- 30-Kato R (1966):** Possible role of P-450 in the oxidation of drugs in liver microsomes. *J. Biochem.*, 59(6): 574-583.
- 31-Kato R and Takanaka A (1968):** Metabolism of drugs in old rats (II) Metabolism in vivo and effects of drugs in old rats. *Jpn. J. Pharmacol.*, 18(4): 389-396.
- 32-Topham JC, McIntosh DAD and Platt DS (1972):** Biochemical changes in rat liver in response to treatment with drugs and other agents. *Biochem. Pharmacol.*, 21(7): 1019-1024.
- 33-Van der Kleijn E (1969):** Kinetics of distribution and metabolism of ataractics of the meprobamate-group in mice. *Arch. Int. Pharmacod. Ther.*, 178(2): 457-480.
- 34-Medical Economics Company (1989):** Physician's desk reference. 43th ed., London. pp: 688-699, 877 and 1523.
- 35-Medical Economics Company (1996):** Physician's desk reference: 50th ed., London. pp: 2674-2675.
- 36-Hassan H, Ghaly E, El-Nashar A and Manggoud H (1988):** Histochemical study on some organs of rats fed rape seed and cotton seed oils. *Egypt. J. Histol.*, 11(2): 247-252.
- 37-Guler G, Turkozer Z, Ozgur E, Tomruk A, Seyhan N and Karasu C (2009):** Protein oxidation under extremely low frequency electric field in guinea pigs. Effect of N-acetyl-L-cysteine treatment. *Gen. Physiol. Biophys.*, 28(1): 47-55.
- 38-Lijnen P, Prihadi JS, van Pelt JF and Fagard RH (2011):** Modulation of reactive oxygen species and collagen synthesis by angiotensin II in cardiac fibroblasts. *The Open Hypertension J.*, 4: 1-17.
- 39-Radwan MA, Essawy AE, Abdelmeguid NE, Hamed SS and Ahmed AE (2008):** Biochemical and histochemical studies on the digestive gland of *Eobania vermiculata* snails treated with carbamate pesticides. *Pestic. Biochem. Physiol.*, 90: 154-167.
- 40-Jeor ST and Ashley JM (1999):** Dietary strategies: issues of diet composition. In: *Obesity: Impact on Cardiovascular Disease*. N.Y.: Futura, Publishing Co. New York, pp: 233-246.
- 41-Al Gahtani S (2006):** Histological and histochemical studies on the effect of two different types of magnetic field on the liver and kidney of Albino rats. M.Sc. Thesis, Faculty of Science, Dammam, K.S.A.
- 42-Abuo El Naga NA and Abd Rabou MA(2012):** The possible protective role of bone marrow transplantation on irradiated mothers and their fetuses. *Stem Cell*, 3(3): 8-30.
- 43- Abdelmeguid NE, Chmaisse HN and Abou NZ (2010):** Silymarin ameliorates Cisplatin-induced hepato-toxicity in rats: histopathological and ultrastructural studies. *Pakistan, J. Biol. Sci., PJBS*, 13(10): 463-479.
- 44-Sakr SA and Okdah YA (2004):** Histological and histochemical alteration induced in the testicular tissue of mice intoxicated with benomyle. *J. Biol. Sci.*, 4(4): 498-500.
- 45-Farrag ARH and Shalby SEM (2007):** Comparative histopathological and histochemical studies on IGR, lufenuron and profenofos insecticide albino rats. *J. Appl. Sci. Res.*, 3(5): 377-386.
- 46-Ramirez-Alvarado M, Merkel JS and Regan L (2000):** A systematic exploration of the influence of the protein stability on amyloid fibril formation in vitro. *PNAS.*, 97 (16): 8979-8984.
- 47- Pulawski W, Ghoshdastider U, Andrisano V and Filipek S (2012):** Ubiquitous amyloid. *Applied Biochem. Biotechnol.*, 166 (7): 1626-1643.
- 48-Kadowaki H (2005):** Amyloid beta induces neuronal cell death through ROS-mediated ASK1 activation. *Cell Death Differ.*, 12(1): 19-24.
- 49- Sakr SA and Shalaby SY (2011):** Ginger extract protects metalaxyl-induced histomorphological and histochemical alterations in testes of albino mice. *J. Appl. Pharm. Sci.*, 1(10): 36-42.